Bioorganic Chemistry 114 (2021) 105099

Contents lists available at ScienceDirect

Bioorganic Chemistry

journal homepage: www.elsevier.com/locate/bioorg

p-Trifluoromethyl- and *p*-pentafluorothio-substituted curcuminoids of the 2,6-di[(*E*)-*benzylidene*)]cycloalkanone type: Syntheses and activities against *Leishmania major* and *Toxoplasma gondii* parasites

Ibrahim S. Al Nasr [a,b], Riadh Hanachi [c], Ridha B. Said [c,d], Seyfeddine Rahali [d,e], Bahoueddine Tangour [e], Siddig I. Abdelwahab [f], Abdullah Farasani [f,g], Manal M. E. Taha [h], Anil Bidwai [g], Waleed S. Koko [b], Tariq A. Khan [i], Rainer Schobert [j], Bernhard Biersack [j,*]

[a] Department of Biology, College of Science and Arts, Qassim University, Unaizah 51911, Saudi Arabia
[b] Department of Science Laboratories, College of Science and Arts, Qassim University, King Abdelaziz Road, Ar Rass 51921, Saudi Arabia
[c] Laboratoire de Caractérisations, Applications et Modélisations des Matériaux, Faculté des Sciences de Tunis, Université de Tunis El Manar, Tunis 2092, Tunisia
[d] Department of Chemistry, College of Science and Arts in Ar Rass, Qassim University, Ar Rass 51921, Saudi Arabia
[e] IPEIEM, Research Unit on Fundamental Sciences and Didactics, Université de Tunis El Manar, Tunis 2092, Tunisia
[f] Medical Research Center, Jazan University, Jazan 45142, Saudi Arabia
[g] College of Applied Medical Sciences, Jazan University, Jazan 45142, Saudi Arabia
[h] Substance Abuse Research Center, Jazan University, Jazan 45142, Saudi Arabia
[i] Department of Clinical Nutrition, College of Applied Health Sciences, Qassim University, Ar Rass 51921, Saudi Arabia
[j] Organic Chemistry Laboratory, University Bayreuth, Universitätsstrasse 30, 95440 Bayreuth, Germany

ARTICLE INFO

Keywords:
Curcumin
Fluorine
Anti-parasitic drugs
Neglected tropical diseases

ABSTRACT

A series of the title curcuminoids with structural variance in the heteroatom of the cycloalkanone and the *p*-substituents of the phenyl rings were tested for their activities against *Leishmania major* and *Toxoplasma gondii* parasites. The majority of them showed high activities against both parasite forms with EC_{50} values in the sub-micromolar concentration range. Bis(*p*-pentafluorothio)-substituted 3,5-di[(*E*)-*benzylidene*]piperidin-4-one **1b** was not just noticeable antiparasitic, but also exhibited a considerable selectivity for *L. major* promastigotes over normal Vero cells. While derivatives differing only in the *p*-phenyl substituents being CF_3 or SF_5 showed similar antiparasitic activities, the cyclic ketone hub was more decisive both for the anti-parasitic activities and the selectivities for the parasites vs. normal cells. QSAR calculations confirmed the observed structure–activity relations and suggested structural variations for a further improvement of the antiparasitic activity. Docking studies based on DFT calculations revealed *L. major* pteridine reductase 1 as a likely molecular target protein of the title compounds.

1. Introduction

Curcumin [1,7-bis(4-hydroxy-3-methoxyphenyl)-1,6-heptadiene-3,5-dione] is the major biologically active constituent of turmeric, a spice made from the roots of *Curcuma longa* which is widely applied in Indian cuisine and traditional Indian medicine [1]. Curcumin has shown significant anticancer activity by addressing various cellular targets involved in cancer cell survival and metastasis. It was found to inhibit or down-regulate NF-κB, COX-2, STAT-3, Akt, and MMP-2 [2–6]. A phase II trial in patients suffering from advanced pancreas tumor diseases revealed a high tolerability of curcumin by all patients, and its biological activity in some patients with pancreatic cancer when administered orally as a monotherapy [7]. As a natural product of a tropical plant, curcumin also has a great potential as a drug against infections and tropical diseases [8,9]. It was tested against various protozoal parasites and it showed activity against *Leishmania*, *Plasmodia* and *Toxoplasma* species [10,11]. Curcumin and certain metal complexes of it displayed activity against *Leishmania major* [12]. In addition, curcumin inhibited glyoxalase 1 of *Toxoplasma gondii* and the proliferation of this parasite *in vitro* [13]. As immune-compromised people are at risk of severe complications when infected with the globally occurring *Toxoplasma gondii* parasites (i.e., the causative agents of toxoplasmosis), new drugs for the treatment of toxoplasmosis in such patients are necessary [14].

* Corresponding author.
E-mail addresses: bernhard.biersack@yahoo.com, bernhard.biersack@uni-bayreuth.de (B. Biersack).

https://doi.org/10.1016/j.bioorg.2021.105099
Received 2 April 2021; Received in revised form 21 May 2021; Accepted 15 June 2021
Available online 17 June 2021

Abbreviations

AmB	Amphotericin B
ATO	Atovaquone
CL	Cutaneous leishmaniasis
DFT	Density functional theory
FBS	Fetal bovine serum
HE	Hydraulic energy
HOMO	Highest occupied molecular orbital
LGA	Lamarckian genetic algorithm
LUMO	Lowest unoccupied molecular orbital
MCL	Mucocutaneous leishmaniasis
MLR	Multiple linear regression
MW	Molecular weight
NTD	Neglected tropical disease
PDB	Protein data bank
POL	Polarizability
PTR1A	Pteridine reductase-1 subunit A
QSAR	Quantitative structure–activity relationship
REF	Molecular refractivity
RPMI	Roswell Park Memorial Institute
SAG	Surface area grid
SI	Selectivity index
TPSA	Topological polar surface area
VL	Visceral leishmaniasis

Leishmaniasis is categorized as a neglected tropical disease (NTD) and clinically subdivided into visceral leishmaniasis (VL), cutaneous leishmaniasis (CL), and mucocutaneous leishmaniasis (MCL). The CL form brought about by various *Leishmania* species such as *L. major*, *L. tropica*, *L. mexicana*, *L. amazonensis* etc., causes severe skin lesions. It is the most prevalent leishmaniasis form responsible for up to 1 million, mostly young, patients annually [15,16]. Although usually not lethal, CL leads to stark and disfiguring skin lesions and to stigmatization of affected persons [17,18]. CL patients are currently treated with pentavalent antimonials, miltefosine, amphotericin or pentamidine [16]. Aside of the general toxicity of clinically applied drugs such as antimonials, another growing problem is the emergence of drug-resistant parasite forms. Thus, new potent anti-parasitic drugs against leishmaniasis are needed.

The efficacy of curcumin as a therapeutic agent for treating human diseases is often hampered by its low bioavailability. Modified curcumin derivatives were reported to have an improved bioavailability and as a consequence a significantly enhanced *in vitro* and in vivo activity compared with curcumin [19]. Fluorinated curcuminoids like EF24 have been reported to be superior to curcumin in the treatment of various cancers (Fig. 1) [20,21]. The monocarbonyl compound EF24 showed improved metabolic stability and bioavailability data when compared with curcumin [22]. Recently, we disclosed new curcuminoids of the 3,5-di[(*E*)-*benzylidene*]piperidin-4-one, or 2,6-di[(*E*)-*benzylidene*]cyclohexanone, or (1*E*,4*E*)-1,5-diphenylpenta-1,4-dien-3-one type, which showed improved anti-tumor activities when compared with EF24 [23,24]. Further modifications with a curtailed curcumin motif included acryl amides, sulfonamides, dioxolanes and thiopyranones [25–27]. However, studies of the anti-parasitic activities of such curcuminoids are rare.

Perfluorinated lipophilic and electron-withdrawing substituents such as CF_3 and SF_5 groups are of particular interest as xenobiotic, chemically stable mimics of negatively charged biomolecules. The SF_5 group was even labelled as 'super trifluoromethyl group' [28]. The synthesis of an 8-pentafluorothio analog of the antimalarial drug mefloquine is a prominent example that showed a higher antimalarial in vivo activity and a longer half-life than mefloquine [28,29]. The enhancing effect of SF_5 substituents on the antitumoral activity of curcuminoids was recently reported [23]. For trifluoromethyl derivatives, promising activities were also observed against *Leishmania* parasites as well as an inhibition of folate enzymes in cancer cells and of analogous pteridine reductase enzymes of *Leishmania* and *Trypanosoma* parasites [30–34]. In the present report, we disclose a series of new and some already known curcuminoids bearing 4-trifluoromethyl or 4-pentafluorosulfanyl substituted phenyl rings, and their promising activities against *L. major* and *T. gondii* parasites (Fig. 1).

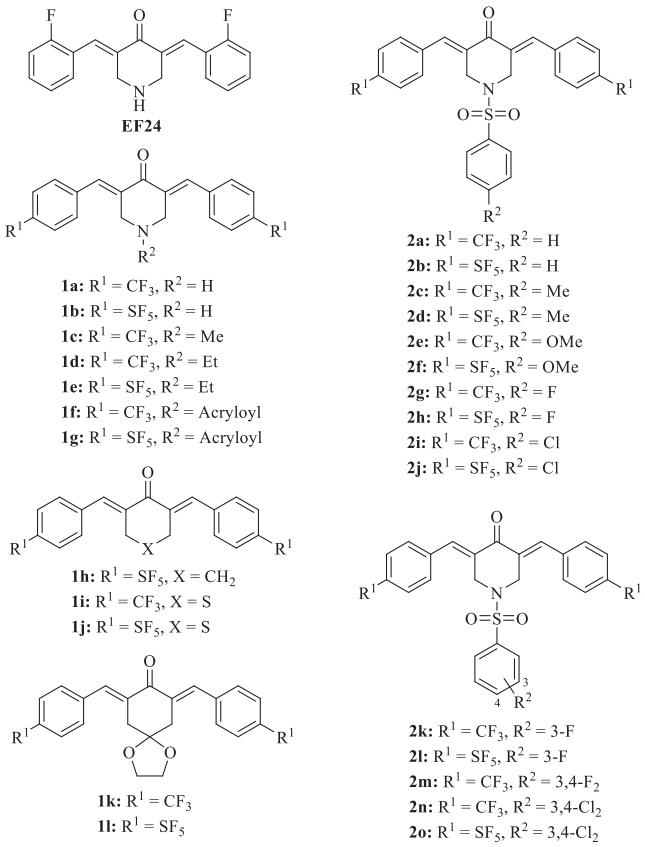

Fig. 1. Structures of curcuminoids EF24, **1a–l**, and **2a–o** used in this study.

2. Results and discussion

EF24 and compounds **1a–l** were prepared from the condensation reaction of one equivalent of the corresponding cyclic ketone with two equivalents of 4-trifluoromethylbenzaldehyde or 4-pentafluorothiobenzaldehyde in MeOH under basic conditions (Scheme 1) [23,26]. Compounds **2a–o** were prepared from the corresponding aryl sulfonamides of 4-piperidinone with 4-trifluoromethyl- or 4-pentafluorothiobenzaldehyde in ethanol under acidic conditions (Scheme 1). The compounds **1a–l** and **2a–o** were obtained as yellow solids in low to moderate yields (30–70%). The structures of all test compounds are provided in detail in Fig. 1. The presented curcuminoids are new except for the compounds **1a**, **1c**, **1e**, **1f**, **1h**, **2a**, and **2c**, which were prepared according to literature procedures [23,26,27].

The curcuminoids **1a–l** and **2a–o** (Fig. 1) were initially tested for

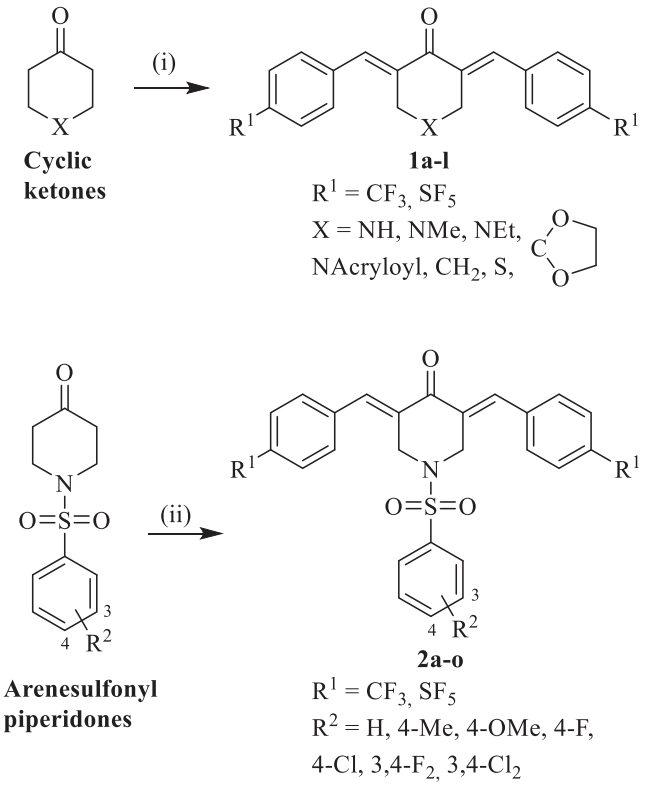

Scheme 1. Reagents and conditions: (i) 4-CF_3-C_6H_4CHO or 4-SF_5-C_6H_4CHO, NaOH, MeOH/H_2O, r.t., 1 h, 31–70%; (ii) 4-CF_3-C_6H_4CHO or 4-SF_5-C_6H_4CHO, conc. HCl, EtOH, reflux, 24 h, 30–41%.

their activity against *T. gondii* tachyzoites (Table 1). Of the compound **1** series, the acrylate **1f** and the thiopyranones **1i** and **1j** showed the highest activity against *T. gondii*, which was also slightly more sensitive to these test compounds than Vero cells. Compound **1j** also showed the highest selectivity index (SI = 5.4) of this group of curcuminoids and it was also more active and selective than EF24. Lower activities were observed for compounds **1a–c** and **1l**, which were less active even than EF24. The series of phenylsulfonamides **2** also comprised very active derivatives against *T. gondii* such as the chlorophenyl derivatives **2i**, **2j**, **2n**, and **2o**, and the 3-fluorophenyl derivatives **2k** and **2l** which were much more active than EF24 and almost as active as atovaquone (ATO). However, these compounds showed no selectivity for parasites over Vero cells. Nevertheless, all test compounds **1** and **2** were more active than the lead curcumin [13].

The activity of compounds **1a–l** and **2a–o** against *L. major* promastigotes and amastigotes was also determined (Table 2). Among the series of compounds **1a–l**, high activities against promastigotes were observed for piperidones **1a–f**, thiopyranone **1i**, and ketals **1k** and **1l** with **1f** and **1l** performin best (EC_{50} = 0.022–0.024 μM). These compounds are much more active against *L. major* promastigotes than curcumin, which was reported to have an EC_{50} value of 103.2 μM [12]. But in most cases, the test compounds were much less active against the amastigotes. Only **1e** also showed a specific activity against the amastigotes. Compounds **1a–c** exhibited considerable selectivities for the promastigotes and the highest selectivity was observed for the new SF_5-substituted compound **1b** (SI = 76). How far the SF_5 group of **1b** actually contributes to the prolonged half-life and increased activity of this compound in *L. major* in vivo models, in analogy to the above mentioned anti-malarial 8-pentafluorothio-mefloquine, remains to be elucidated. Compounds **1f**, **1i**, **1k** and **1l** also showed distinct selectivities for the promastigotes. Among the compounds of the **2a–o** series, the highest activities were observed for **2a**, **2c**, **2e–h**, and **2 k–m**. A considerable selectivity was found for **2m** (SI = 19.2). The determined specificity indices (SPI, specificity for promastigotes vs. amastigotes) for the test compounds also underline the high specificity of many tested curcuminoids for promastigotes when compared with their activities against amastigotes. Compared with the positive control amphotericin B (AmB), all tested curcuminoids showed distinctly higher activities against the promastigotes. The lowest SPI values (i.e., the highest specificities for promastigotes) of 0.002–0.003 were observed for compounds **1b-d**, **2e** and **2m**. This is remarkable because in contrast to that, many approved antileishmanial drugs display a high activity against amastigotes, and other drug candidates show a higher activity against *L. major* amastigotes than against promastigotes [35,36]. AmB with an SPI of 1.766 is also more active against amastigotes than against promastigotes, however, compounds with SPI < 2 can be considered as active against both promastigotes and amastigotes.

The dependence of the measured activities on the presence and influence of the CF_3 or SF_5 groups remained obscure. Sometimes, CF_3 analogs were more active, yet very often there was no distinct difference among compounds with the same central cyclic ketone fragment. In contrast, the substitution pattern of the central cyclic ketone scaffold was found to be decisive for high activity and selectivity or lack of activity in certain cases. The sulfonamides **2a–o** were generally more active against *T. gondii* than EF24 and most of the curcuminoids of the **1a–l** series. Only acrylate **1f** and thiopyranones **1i** and **1j** reached the activities of the sulphonamides here. It seems that a carbonamide or sulfonamide function is crucial for high activity. The sulfur atoms of the thiopyranones **1i** and **1j** might form H-bonds (as acceptors) or can be

Table 1
Inhibitory concentrations IC_{50} (in μM) of test compounds **1a–l** and **2a–o** when applied to cells of the Vero (African green monkey kidney epithelial) cell line, effective concentrations EC_{50} when applied to cells of *Toxoplasma gondii*.[a] Amphotericin B (AmB, Vero) and atovaquone (ATO, Vero and *T. gondii*) were applied as positive controls for the indicated cells.

Compd.	EC_{50} (*T. gondii*)	IC_{50} (Vero)	SI (Vero / *T. gondii*)[b]
1a	0.95	1.41	1.48
1b	1.33	2.28	1.71
1c	0.99	1.88	1.90
1d	0.48	1.14	2.38
1e	0.72	1.89	2.63
1f	0.22	0.41	1.86
1g	0.67	0.77	1.15
1h	0.40	0.70	1.75
1i	0.28	1.10	3.93
1j	0.15	0.81	5.40
1k	0.51	0.68	1.33
1l	1.61	0.53	0.33
2a	0.22	0.27	1.23
2b	0.20	0.27	1.35
2c	0.32	0.39	1.22
2d	0.24	0.41	1.71
2e	0.29	0.36	1.24
2f	0.26	0.29	1.12
2g	0.37	0.33	0.89
2h	0.26	0.31	1.19
2i	0.15	0.12	0.80
2j	0.10	0.07	0.70
2k	0.14	0.11	0.79
2l	0.10	0.06	0.60
2m	0.39	0.46	1.18
2n	0.11	0.15	1.36
2o	0.10	0.09	0.90
EF24	0.68	1.22	1.79
Curcumin	38.3[c]	–	–
AmB	–	7.7	–
ATO	0.07	9.5	136

[a] Values are the means of at least three independent experiments (SD ± 15%). They were obtained from concentration–response curves by calculating the percentage of treated cells in comparison to untreated controls after 72 h. [b]Selectivity index SI (IC_{50}/EC_{50}) was calculated from the corresponding IC_{50} values for the Vero cells and the EC_{50} values against *T. gondii*. [c]Value was taken from Goo et al. [13].

Table 2
Effective concentrations EC_{50} (in μM) of test compounds **1a–l** and **2a–o** when applied to promastigotes and amastigotes of *Leishmania major*.[a] Amphotericin B (AmB) was applied as a positive control.

Compd.	EC_{50} promastigotes	EC_{50} amastigotes	SPI[b]	SI Vero / promastigotes[c]	SI Vero / amastigotes[c]
1a	0.037	3.16	0.012	38.1	0.45
1b	0.030	13.7	0.002	76	0.17
1c	0.040	17.2	0.002	47	0.11
1d	0.041	13.0	0.003	27.8	0.09
1e	0.035	0.72	0.049	54	2.63
1f	0.022	2.79	0.008	18.6	0.15
1g	0.103	8.60	0.012	7.5	0.09
1h	0.158	11.6	0.014	4.43	0.06
1i	0.047	2.10	0.022	23.4	0.52
1j	0.110	2.02	0.054	7.36	0.40
1k	0.030	2.43	0.012	22.7	0.28
1l	0.024	1.90	0.013	22.1	0.28
2a	0.022	2.00	0.011	12.3	0.14
2b	0.066	7.79	0.008	4.1	0.04
2c	0.030	2.48	0.012	13.0	0.16
2d	0.111	2.05	0.054	3.69	0.20
2e	0.024	9.97	0.002	15	0.04
2f	0.026	3.01	0.009	11.2	0.10
2g	0.023	3.69	0.006	14.4	0.09
2h	0.025	3.21	0.008	12.4	0.10
2i	0.072	10.1	0.007	1.67	0.01
2j	0.093	2.28	0.041	0.75	0.03
2k	0.023	3.69	0.006	4.79	0.03
2l	0.022	2.19	0.010	2.72	0.03
2m	0.024	10.2	0.002	19.2	0.05
2n	0.126	1.45	0.087	1.19	0.1
2o	0.110	8.01	0.014	0.82	0.01
EF24	0.28	19.9	0.014	4.36	0.06
AmB	0.83	0.47	1.766	9.6	16.4

[a] Values are the means of three experiments (SD ± 15%). They were obtained from concentration–response curves by calculating the percentage of treated cells in comparison to untreated controls after 72 h. [b]Specificity index SPI for promastigotes vs. amastigotes was calculated from the EC_{50} values of promastigotes and amastigotes. [c]Selectivity index SI (IC_{50}/EC_{50}) was calculated from the corresponding IC_{50} values for the Vero cells (Table 1) and the EC_{50} values against *L. major*.

oxidised to sulfones in the cells, mimicking the sulfonamides of compounds **2a–o**. Concerning the arene substituents of compounds **2a–o**, 3-fluoro-, 4-chloro-, and 3,4-dichlorophenylsulfonamides led to the highest activities against *T. gondii*.

The following structure activity-relationships for the compounds **1a–l** and **2a–o** were identified from the results in *L. major* parasites: The SF_5 derivatives **1g**, **1h** and **1j** showed relatively low activities against the *L. major* promastigotes indicating a negative role for the SF_5 group in combination with *N*-acryloylpiperidone, cyclohexanone and thiopyranone scaffolds. However, compound **1i**, the CF_3 analog of **1j**, displayed reasonable activity and selectivity, and also showed high activity against *T. gondii*. High activity and considerable selectivity were identified for compounds **1a–e** indicating a crucial role of the unmodified piperidone and the *N*-(m)ethylpiperidone scaffolds to effectuate *L. major* promastigote selectivity (Fig. 2). Only the *N*-ethyl derivative **1e** showed activity at submicromolar concentrations against the *L. major* amastigotes which is a hint at the possible positive role of more hydrophobic *N*-alkyl substituents for the future design of more active analogs against *L. major* amastigotes. The phenylsulfonamide derivatives **2a–o**, SF_5 derivatives **2d** and **2j** were less active than their congeners, and the combination of SF_5 substitution with toluene- or 4-chlorosulfonamide central scaffolds led to a reduced efficacy. In addition, 3,4-dichlorophenylsulfonamides **2n** and **2o** showed a distinctly lower activity than the other compound **2** analogs. Some selectivity was observed for compounds **2g**, **2h**, and **2m**. Hence, a central 4-fluorophenyl or 3,4-difluorophenylsulfonyl piperidone moiety apparently correlated with a better selectivity for promastigotes while the 3-fluoro- and 4-chlorophenyl congeners **2i–l** showed only lesser selectivities.

In addition to Vero cells, the effects of selected test compounds on macrophages were investigated in order to obtain more information about the selectivity of the test compounds for the tested parasites (Table 3). Compound **1b** showed the lowest growth inhibitory activity against macrophages of the tested compounds. **1b** already showed the

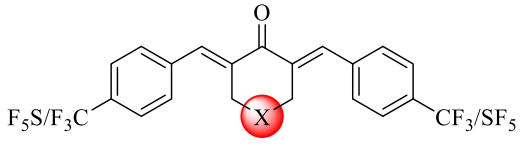

Activity against *T. gondii*:
X = N-Acryloyl (**1f**/CF_3)
X = S (**1i**, **1j**)

Activity against *L. major*:
X = N-H/Me/Et (**1a-f**)
X = S (**1i**/CF_3)
X =  (**1k**, **1l**)

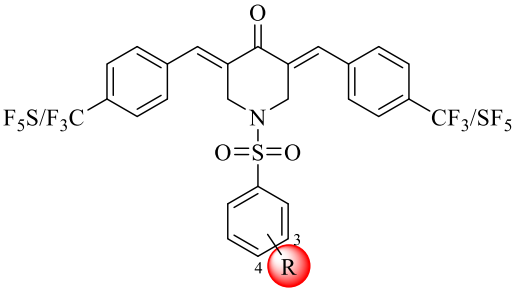

Activity against *T. gondii*:
R = 3-F (**2k**, **2l**), 4-Cl (**2i**, **2j**), 3,4-Cl_2 (**2n**, **2o**)

Activity against *L. major*:
R = H (**2a**/CF_3), 4-Me (**2c**/CF_3), 4-OMe (**2e**, **2f**), 4-F (**2g**, **2h**), 3-F (**2k**, **2l**), 3,4-F_2 (**2m**)

Fig. 2. Structure-activity relationships of curcuminoids **1a–l** and **2a–o**.

Table 3
Inhibitory concentrations IC_{50} (in μM) of selected test compounds **1** and **2** when applied to macrophages and selectivity indices (SI) of the test compounds.

Compd.	IC_{50} macrophages[a]	SI macrophages / *T. gondii*[b]	SI macrophages / amastigotes[b]	SI macrophages / promastigotes[b]
1a	3.65	3.84	1.15	99
1b	16.50	12.4	1.21	550
1j	4.04	26.9	2.0	37
1k	2.99	5.86	1.23	100
1l	2.57	1.60	1.35	107
2a	1.63	7.41	0.82	74
2c	3.18	9.94	1.29	106
2d	3.08	12.8	1.5	28
2l	1.02	10.2	0.47	46
2n	1.13	10.3	0.78	8.97

[a] Values are the means of three repeated experiments (SD ± 15%). They were obtained from concentration–response curves by calculating the percentage of treated cells in comparison to untreated controls after 72 h. [b]Selectivity index (IC_{50}/EC_{50}) calculated from the corresponding IC_{50} values for the macrophages and the EC_{50} values from *T. gondii* and *L. major* (pro- and amastigotes).

lowest activity against the Vero cells. Consequently, **1b** has a high selectivity for *L. major* promastigotes (SI = 550) and a considerable selectivity for *T. gondii* cells (SI = 12.4). The highest selectivity for *T. gondii* was observed for compound **1j** (SI = 26.9). Due to the low activity of the tested compounds against *L. major* amastigotes, the selectivity for amastigotes is only marginal, compared with their activities against macrophages.

In order to establish a rationale for the observed structure–activity relations, i.e., a mathematical connection between biological activity expressed in terms of pIC_{50} and physicochemical and structural properties of the test compounds, we used a Quantitative Structure-Activity Relationships (QSAR) approach [37]. This method implies a prediction of the pharmacological activities of the test compounds by processing their molecular parameters (a.k.a. descriptors), either measured or calculated, e.g. via density functional theory (DFT), in a quantitative model based on multiple linear regression (MLR). This combined QSAR-DFT approach allows to build simple (less parameterized) models [38–40]. First, the geometries of all compounds were optimized using B3LYP with the 6–311 + G(d,p) basis set (cf. Supporting Information, Figure S1). Based upon these geometries, the following descriptors were calculated or deduced. HOMO and LUMO energies, the ctanol-water partition coefficient ($log_{10}P$), molar weight (MW), polarizability (POL), surface area grid (SAG), hydraulic energy (HE), molecular refractivity (REF), volume (V), topological polar surface area (TPSA), number of atoms (nATOMS), hydrogen bond acceptors (nON, counting all N and O atoms), hydrogen bond donor (nOHNH, counting the sum of all NH and OH groups), number of rotatable bonds (nROTB), total electronic energy E and dipolar moment μ (*cf.* SI, Table S1).

Table S1 shows that compound **2o** has a large logP value of 8.73, which corresponds to the large values of SAG (766.57 $Å^3$), MW (736.48 g/mol), MR (144.23 $Å^3$), V (1409.9 A^3) and nATOMS (44) and the smallest HOMO energy (-0.27187 a.u.). Compound **1a** had the smallest value of logP (5.66) which corresponds to the smallest values of SAG (601.21 $Å^3$), MW (411.35 g/mol), MR (99.41 $Å^3$), Vol (1011.75 A^3) and nATOMS (29) and associates with the smallest dipolar moment (0.35 Debye). TPSA values were in the range of 17.07 – 63.69 $Å^2$, which were still within the acceptable range (<140 $Å^2$) to have a high oral absorption. The number of rotatable bonds lay between 4 and 6 for all compounds. **2f** has the largest HE value (7.45 kcal/mol) while the smallest HE value was calculated for **1d** (1.63 kcal/mol).

For validation of the QSAR model, different statistical parameters were used:

- The cross-validity coefficient R^2_{CV} (LOO) was used to estimate the internal validity of the model. The threshold for approval is R^2_{CV} (LOO) greater than 0.5 [41].
- For a positive external validation, the quadratic correlation coefficient R^2_{ext} should be greater than 0.6 [42].
- Significance $P < 0.05$.

The compounds were divided into two groups for each experimental activity: 21 compounds were used as a training set (internal validation) and six compounds were used for the external test (external validation). The measured and predicted activities and residual values are presented in Table S2 (*cf.* SI).

The values of compounds denoted with boldfaced numbers were not used to build the models nor for the external validation.

The following equations show meaningful results of association analyses between the curcuminoid's activities and their calculated descriptors:

$$EC50(T.gondii) = 1.68421669 - 0.05004291*TPSA + 0.8481162*nON + 0.44750966*nOHNH - 0.35542755*nROTB \quad (1)$$

$$IC50(Vero) = 11.03542873 + 29.78379959*HOMO - 0.24482523*POL + 0.06420943*REF + 0.59274826*nOHNH \quad (2)$$

$$EC50(promastigotes) = -0.22486011 + 0.044368*logP - 0.00249733*TPSA + 0.01339477*nROTB \quad (3)$$

From Eq. (1) and Eq. (2), the coefficients of nOHNH are positive, which indicate a promoter effect of weak bonding between curcuminoid derivatives and parasite. The positive coefficient of the octanol–water partition coefficient (logP) in Eq. (3) is in line with the increased biological activity of more lipophilic curcuminoid derivatives.

Overall, a good correlation between experimental data and predicted biological activities was obtained (Fig. 3) with high values of R^2_{cv} (0.72, 0.84, and 0.60 for EC_{50} (*T. gondii*), IC_{50} (Vero), and EC_{50} (promastigotes), respectively). The R^2_{ext} values (0.85, 0.81, and 0.88 for EC_{50} (*T. gondii*), IC_{50} (Vero), and EC_{50} (promastigotes), respectively) confirm these results.

Protozoan parasites like *Leishmania* depend on exogenous pteridine sources (folates and pterins). Upon uptake by the parasite, these pteridines are reduced to bioactive tetrahydro-forms by parasite enzymes. Pteridine reductase-1 (PTR1) of *L. major* is one of the enzymes involved in parasitic pteridine reduction [43,44] and, thus, a suitable drug target for treating *L. major* infections. We carried out docking experiments with the curcuminoids **1i** and EF24. The active site of the *L. major* PTR1 harbors crucial hydrogen donating amino acid residues (e.g., tyrosines), which can interact with hydrogen acceptors such as fluorine of **1i** and EF24 [44]. All binding parameters of **1i** and EF24 obtained after docking with PTR1A are listed in Table 4. Estimated total free energy of binding of the two ligands was −8.12 ± 0.12 and −9.16 ± 0.14 kcal/mol (values are mean ± SD of 20 docking runs), respectively. The estimated K_i values were 1.02 μM and 0.18 μM, respectively (values calculated for lowest energy docking run out of 20 runs). The total free energy of binding (and hence the Ki) estimated for **1i** and EF24 suggests a considerable affinity.

The two ligands appear to bind at separate sites of the enzyme (Fig. 4). The strong inhibition by **1i** can be explained by its binding to the active site of the enzyme, which would interfere with substrate binding (see below). In contrast, EF24 appears to bind outside the substrate binding pocket. Therefore, in spite of strong binding, it may be unable to block the substrate binding site, which would explain the reduced experimental parasite growth inhibition by EF24.

An analysis of docked complexes of the two compounds was done using LigPlot + software. LigPlots are shown in Figures 5 and S2. LigPlot analysis of the docked complexes of the ligands with PTR1A revealed several significant interactions of the ligands with PTR1A. The ligands

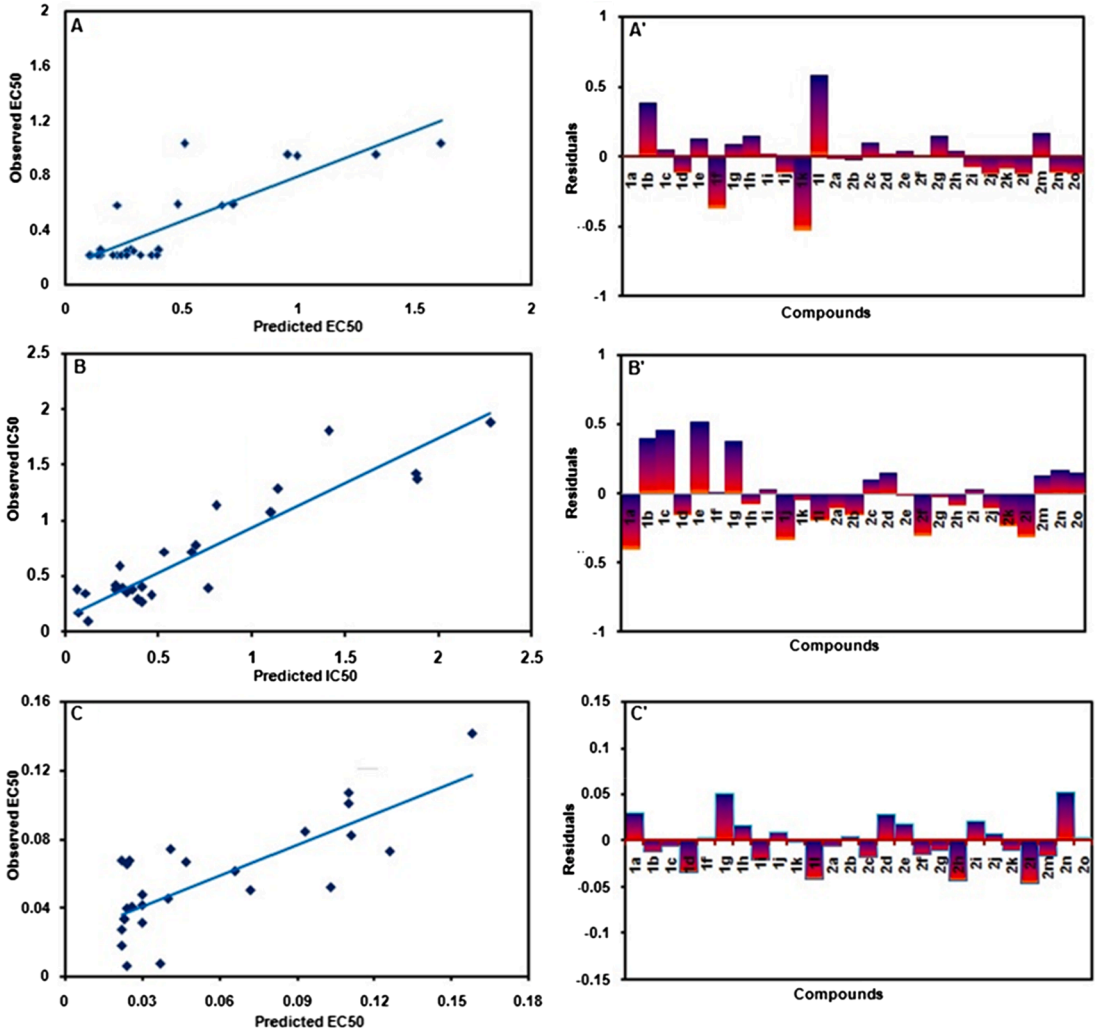

Fig. 3. Generic leverage plot of experimental versus corresponding predicted activities {EC_{50} (*T. gondii*) (**A**), IC_{50} (Vero) (**B**) and EC_{50} (promastigotes) (**C**)} and diagram of residual values {EC_{50} (*T. gondii*) (**A'**), IC_{50} (Vero) (**B'**) and EC_{50} (promastigotes) (**C'**)}.

Table 4
Interaction energies and inhibitor constants (K_i) for the binding of **1i** and EF24 to pteridine reductase – A subunit (PTR1A) (values for the lowest energy conformation from 20 docking runs).

Parameters	1i	EF24
vdW + H-bond + desolvation energy (kcal/mol)	−9.83	−8.51
Electrostatic energy (kcal/mol)	+0.16	−1.58
Final total internal energy (kcal/mol)	0.00	−0.61
Torsional free energy (kcal/mol)	+1.49	+0.89
Estimated free binding energy (kcal/mol)	−8.18	−9.20
Estimated inhibition constant K_i (μM, 298.15 K)	1.02	0.18

appear to bind in extended conformations and make extensive van der Waals contacts with certain enzyme residues (Figures 5 and S2). **1i** established four H-bonds with active site residues of the protein. The carbonyl group of **1i** formed H-bonds with the carboxamide of the Asn-109 side-chain and with the backbone NH of Gly-19. The interaction of **1i** with the phenolic hydroxyl group of Tyr-194 occurred via one of its CF_3 groups while the opposite CF_3 group interacted with the backbone NH of His-38. Tyr-194 is crucial for the interaction with and the first-step reduction of the pterin substrate to the dihydro form and builds a catalytic triad with Lys-198 and Asp-181 in *L. major* PTR1 for this reason [44]. Various known PTR1 inhibitors were shown to interact with these residues and to block substrate binding to the active site, which

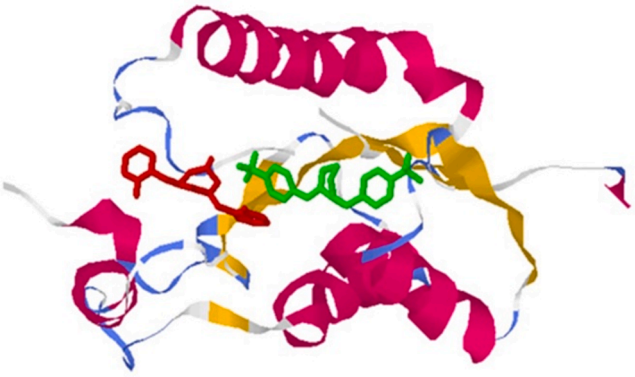

Fig. 4. Optimized structures of selected curcuminoids. Partial structure of PTR1 subunit A (pdb file 1E92). Helices are shown in pink, beta structures in yellow and bends in blue. Figure shows **1i** (green) and EF24 (red) bound to PTR1A. (For interpretation of the references to colour in this figure legend, the reader is referred to the web version of this article.)

underlines the importance of the described H-bond interaction by **1i** [33,44,45]. In the case of the PTR1 inhibitor methotrexate, for instance, the replacement of the oxo group of the pteridine ring of folic acid by an

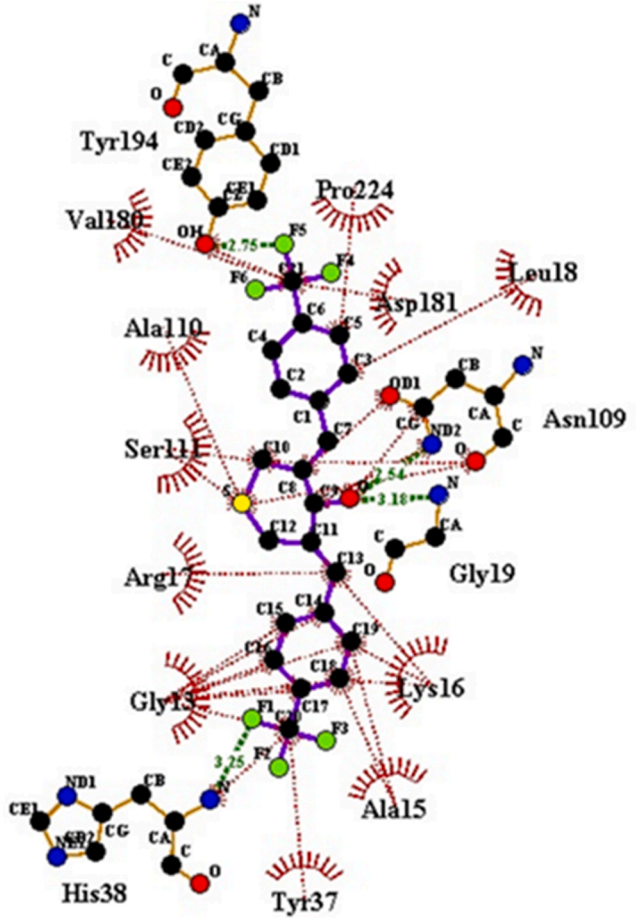

Fig. 5. LigPlot of **1i** interactions with residues of PTR1A. Ligand and residue atoms are shown in CPK colors. Residues are numbered. Hydrogen bonds are shown with green dotted lines and hydrophobic interactions with red dotted rays. (For interpretation of the references to colour in this figure legend, the reader is referred to the web version of this article.)

additional amino group in the methotrexate molecule is crucial for the inhibitory activity of methotrexate based on the H-bond of this amino group with Tyr-194 [44]. **1i** also established extensive hydrophobic contacts with a number of amino acids of the active site, namely Gly-13, Ala-15, Lys-16, Arg-17, Leu-18, Tyr-37, Asp-181, Asn-109, Ala-110, Ser-111, Val-180 and Pro-224. The hydrophobic interaction with Asp-181 of the already mentioned catalytic triad (together with Tyr-194 and Lys-198) is of particular interest. The reference compound EF24 formed two H-bonds with Asp-181 and Tyr-283, respectively. The H-bond with Tyr-283 was formed by one of the fluorines of the EF24 molecule while the piperidone NH group established the second H-bond with the carboxylate group of Asp-181. In addition, hydrophobic interactions of EF24 were seen with Arg-17, Leu-18, Asp-181, Met-183, Gln-186, Leu-188, Pro-224, Gly-225, Leu-226, Ser-227 and Tyr-283.

3. Conclusions

Promising results were obtained from the evaluation of a series of curcuminoids as potential drugs against pathogenic parasites such as *T. gondii* and *L. major*, which can cause severe infections in humans. Both high activities against and considerable selectivities for the parasites were discovered. More detailed research about the mechanisms of action is warranted in order to identify the reason for these peculiar effects. The *L. major* pteridine reductase 1 might be a possible drug target as to docking results. It is remarkable that the new SF_5 derivative **1b** showed considerable selectivity for *L. major* promastigotes. Investigational applications of some of the tested curcuminoids for the treatment of cutaneous leishmaniasis in *in vivo* models (i.e., *L. major* infection) appear promising. Feasible combinations of the most active curcuminoids with approved anti-parasitic drugs can be useful in order to optimize their efficacy, and to reduce the minimal effective dosage and possible side-effects in future animal studies.

4. Experimental

4.1. Chemistry

Compounds **1a**, **1c**, **1e**, **1f**, **1h**, **2a**, and **2c** were prepared following literature procedures and analyzed. The obtained analytical data was in line with published data of these compounds [23–27]. Synthetic procedures and analytical data of the new derivatives are given below. All starting compounds were purchased from the usual retailers and used without further purification. Column chromatography: silica gel 60 (230–400 mesh). Melting points (uncorrected), Electrothermal 9100; NMR spectra, Bruker Avance 300 spectrometer; chemical shifts are given in parts per million (δ) downfield from tetramethylsilane as internal standard; Mass spectra, Thermo Finnigan MAT 8500 (EI). Elemental analysis were carried out with an Elementar UNICUBE (Elementar Analysensysteme GmbH).

4.1.1. (3E,5E)-3,5-Bis-(4-pentafluorothiobenzylidene)-piperidine-4-one (1b)

4-Piperidinone monohydrate hydrochloride (153 mg, 1.0 mmol) and 4-(pentafluorothio)benzaldehyde (464 mg, 2.0 mmol) were dissolved in MeOH (10 mL) and NaOH (40 mg) in H_2O (1 mL) was added. The reaction mixture was stirred at room temperature for 2 h. The formed precipitate was collected, washed with MeOH/H_2O and dried in vacuum. Yield: 366 mg (0.70 mmol, 70%); yellow solid of m.p. 90–92 °C; υ_{max}(ATR)/cm^{-1} 2936, 1679, 1617, 1598, 1496, 1410, 1325, 1302, 1253, 1206, 1181, 982, 821, 794, 733, 663; ^{1}H NMR (300 MHz, DMSO-d_6) δ 4.00 (4H, s), 7.61 (2H, s), 7.7–7.8 (4H, m), 7.9–8.0 (4H, m); ^{13}C NMR (75.5 MHz, DMSO-d_6) δ 47.3, 56.6, 126.0, 131.0, 132.3, 136.8, 138.4, 152.3, 187.6; *m/z* (%) 527 (70) [M$^+$], 499 (63), 247 (100), 231 (77), 115 (57); Anal. Calcd. for $C_{19}H_{15}F_{10}NOS_2$: C, 43.27; H, 2.87; N, 2.66. Found: C, 43.10; H, 2.93; N, 2.59.

4.1.2. (3E,5E)-3,5-Bis-(4-trifluoromethylbenzylidene)-1-ethylpiperidine-4-one (1d)

N-Ethylpiperidin-4-one (95 mg, 0.75 mmol) and 4-trifluoromethylbenzaldehyde (258 mg, 1.5 mmol) were dissolved in MeOH (10 mL) and NaOH (40 mg, dissolved in H_2O) was added. The reaction mixture was stirred at room temperature for 1 h. The formed precipitate was collected, washed with MeOH and dried in vacuum. Yield: 100 mg (0.23 mmol, 31%); yellow solid of m.p. 205–206 °C; υ_{max}(ATR)/cm^{-1} 2986, 2785, 1675, 1615, 1593, 1416, 1326, 1259, 1162, 1111, 1070, 1015, 990, 932, 844, 699; ^{1}H NMR (300 MHz, $CDCl_3$) δ 1.04 (3H, t, J = 7.1 Hz), 2.60 (2H, q, J = 7.1 Hz), 3.78 (4H, s), 7.48 (4H, d, J = 8.2 Hz), 7.67 (4H, d, J = 8.2 Hz), 7.80 (2H, s); ^{13}C NMR (75.5 MHz, $CDCl_3$) δ 12.3, 51.3, 54.2, 122.1, 125.5–125.7 (m), 130.1, 130.3, 130.5, 130.9, 135.0, 138.6, 186.9; *m/z* (%) 439 (91) [M$^+$], 411 (38), 252 (30), 226 (37), 173 (43), 145 (43), 97 (60), 83 (69), 69 (60), 61 (100), 43 (79); Anal. Calcd. for $C_{23}H_{19}F_6NO$: C, 62.87; H, 4.36; N, 3.19. Found: C, 62.78; H, 4.29; N, 3.24.

4.1.3. (3E,5E)-3,5-Bis-(4-pentafluorothiobenzylidene)-1-acryloylpiperidone (1g)

1b (100 mg, 0.19 mmol) was suspended in acetone and treated with acryloyl chloride (35 μL, 0.43 mmol). K_2CO_3 (197 mg, 1.43 mmol, dissolved in 2 mL H_2O) was added and the reaction mixture was stirred at room temperature for 24 h. Water (20 mL) was added and the formed precipitate was collected, washed with water and dried in vacuum. Yield: 68 mg (0.12 mmol, 63%); yellow solid of m.p. 99–100 °C;

υ_{max}(ATR)/cm^{-1} 2934, 1647, 1616, 1496, 1440, 1410, 1295, 1262, 1231, 1209, 1191, 1170, 1135, 1100, 976, 827, 799, 739, 665; ^{1}H NMR (300 MHz, $CDCl_3$) δ 4.76 (4H, s), 5.6–5.7 (1H, m), 6.2–6.3 (2H, m), 7.4–7.6 (4H, m), 7.7–7.9 (6H, m); ^{13}C NMR (75.5 MHz, $CDCl_3$) δ 46.0, 125.7, 126.4, 126.7, 129.1, 129.7, 130.2, 133.5, 137.6, 154.1, 165.5, 185.8; *m/z* (%) 581 (82) [M$^+$], 526 (30), 115 (25), 55 (100); Anal. Calcd. for $C_{22}H_{17}F_{10}NO_2S_2$: C, 45.44; H, 2.95; N, 2.41. Found: C, 45.32; H, 2.99; N, 2.48.

4.1.4. (3E,5E)-3,5-Bis-(4-trifluoromethylbenzylidene)-tetrahydrothiopyran-4-one (**1i**)

Tetrahydro-4H-thiopyran-4-one (116 mg, 1 mmol) and 4-trifluoromethylbenzaldehyde (348 mg, 2.0 mmol) were dissolved in methanol (10 mL) and NaOH (200 mg, dissolved in 2 mL H_2O) was added. The reaction mixture was stirred at room temperature for 1 h. The formed precipitate was collected and dried in vacuum. Yield: 150 mg (0.35 mmol, 35%); yellow solid of m.p. 152–153 °C; υ_{max}(ATR)/cm^{-1} 2886, 1662, 1606, 1581, 1410, 1322, 1276, 1194, 1165, 1118, 1068, 1016, 983, 963, 918, 855, 834, 750, 732, 669, 632; ^{1}H NMR (300 MHz, DMSO-d_6) δ 4.00 (4H, s), 7.65 (2H, s), 7.24 (4H, d, J = 8.3 Hz), 7.82 (4H, d, J = 8.3 Hz); ^{13}C NMR (75.5 MHz, DMSO-d_6) δ 29.1, 122.2, 125.4, 125.8, 128.2, 128.6, 129.1, 129.4, 130.5, 130.8, 133.6, 136.2, 138.6, 156.0, 188.1; *m/z* (%) 428 (62) [M$^+$], 359 (43), 215 (27), 184 (62), 147 (38), 115 (100); Anal. Calcd. for $C_{21}H_{14}F_6OS$: C, 58.88; H, 3.29. Found: C, 58.79; H, 3.21.

4.1.5. (3E,5E)-3,5-Bis-(4-pentafluorothiobenzylidene)-tetrahydrothiopyran-4-one (**1j**)

Tetrahydrothiopyran-4-one (31 mg, 0.27 mmol) and 4-(pentafluorothio)benzaldehyde (124 mg, 0.54 mmol) were dissolved in MeOH (5 mL). NaOH (20 mg, 0.5 mmol) and H_2O (1 mL) were added and the reaction mixture was stirred at room temperature for 1 h. The formed precipitate was collected, washed with MeOH/H_2O and dried in vacuum. Yield: 45 mg (0.083 mmol, 31%); yellow solid of m.p. 180–181 °C; υ_{max}(ATR)/cm^{-1} 1661, 1609, 1580, 1493, 1424, 1406, 1317, 1278, 1199, 1185, 1139, 1101, 986, 922, 824, 811, 765, 741, 678, 658; ^{1}H NMR (300 MHz, $CDCl_3$) δ 3.84 (4H, s), 7.45 (4H, d, J = 8.4 Hz), 7.7–7.9 (6H, m); ^{13}C NMR (75.5 MHz, $CDCl_3$) δ 29.9, 126.3, 126.4, 129.8, 129.9, 134.7, 135.8, 138.3, 153.2, 188.2; *m/z* (%) 544 (100) [M$^+$], 417 (65), 242 (55), 147 (24), 115 (36); Anal. Calcd. for $C_{19}H_{14}F_{10}O_2S_3$: C, 41.91; H, 2.59. Found: C, 41.79; H, 2.66.

4.1.6. (7E,9E)-7,9-Bis-(4-trifluoromethylbenzylidene)-1,4-dioxaspiro[4.5]decan-8-one (**1k**)

1,4-Cyclohexanedione monoethylene acetal (156 mg, 1 mmol) and 4-trifluoromethylbenzaldehyde (348 mg, 2.0 mmol) were dissolved in methanol (10 mL) and NaOH (200 mg, dissolved in 2 mL H_2O) was added. The reaction mixture was stirred at room temperature for 1 h. The formed precipitate was collected and dried in vacuum. Yield: 150 mg (0.32 mmol, 32%); yellow solid of m.p. 172–173 °C; ν_{max} (ATR)/cm^{-1}: 3047, 29645, 2896, 1677, 1615, 1587, 1414, 1324, 1267, 1232, 1195, 1154, 1113, 1068, 1043, 1015, 987, 948, 936, 920, 895, 850, 836, 822, 769, 736, 699, 638; ^{1}H NMR (300 MHz, DMSO-d_6): δ 3.1–3.2 (4H, m), 3.8–3.9 (4H, m), 7.7–7.9 (10*H*, m); ^{13}C NMR (75 MHz, DMSO-d_6): δ 37.1, 64.3, 105.8, 122.2, 125.4, 125.8, 129.0, 130.8, 135.0, 135.8, 138.9, 187.2; *m/z* (%) 468 (100) [M$^+$], 255 (22), 183 (54), 115 (88), 86 (27); Anal. Calcd. for $C_{24}H_{18}F_6O_3$: C, 61.54; H, 3.87. Found: C, 61.43; H, 3.95.

4.1.7. (7E,9E)-7,9-Bis-(4-pentafluorothiobenzylidene)-1,4-dioxaspiro[4.5]decan-8-one (**1l**)

1,4-Cyclohexanedione monoethylene acetal (88 mg, 0.5 mmol) and 4-(pentafluorothio)benzaldehyde (232 mg, 1.0 mmol) were dissolved in methanol (10 mL) and NaOH (200 mg, dissolved in 2 mL H_2O) was added. The reaction mixture was stirred at room temperature for 1 h. The formed precipitate was collected and dried in vacuum. Yield: 180 mg (0.31 mmol, 31%); yellow solid of m.p. 195–197 °C; ν_{max} (ATR)/cm^{-1}: 2956, 2899, 1670, 1614, 1583, 1496, 1408, 1343, 1321, 1294, 1265, 1240, 1188, 1154, 1096, 7044, 1008, 988, 947, 825, 803, 760, 732, 704, 664, 633; ^{1}H NMR (300 MHz, DMSO-d_6): δ 3.1–3.2 (4H, m), 3.8–3.9 (4H, m), 7.7–7.8 (6H, m), 7.9–8.0 (4H, m); ^{13}C NMR (75 MHz, DMSO-d_6): δ 37.1, 64.3, 105.8, 122.2, 126.0, 130.9, 135.1, 135.5, 138.8, 152.2–152.6 (m), 187.1; *m/z* (%) 584 (100) [M$^+$], 313 (21), 241 (19), 115 (55), 86 (23); Anal. Calcd. for $C_{22}H_{18}F_{10}O_3S_2$: C, 45.21; H, 3.10. Found: C, 45.12; H, 3.04.

4.1.8. (3E,5E)-3,5-Bis-(4-pentafluorothiobenzylidene)-1-(benzenesulfonyl)-piperidone (**2b**)

1-(Benzolsulfonyl)-4-piperidinone (140 mg, 0.79 mmol) and 4-(pentafluorothio)-benzaldehyde (348 mg, 1.5 mmol) were dissolved in EtOH (10 mL) and conc. HCl (1 mL) was added. The reaction mixture was refluxed for 24 h. After cooling down to room temperature, the formed precipitate was collected, washed with EtOH and dried in vacuum. Yield: 160 mg (0.24 mmol, 30%); yellow solid of m.p. 237–238 °C; υ_{max}(ATR)/cm^{-1} 1676, 1612, 1591, 1573, 1496, 1447, 1409, 1354, 1297, 1244, 1208, 1184, 1169, 1099, 1036, 983, 962, 933, 837, 824, 799, 762, 750, 732, 721, 694, 665; ^{1}H NMR (300 MHz, DMSO-d_6) δ 4.67 (4H, s), 7.5–7.6 (6H, m), 7.6–7.8 (5H, m), 8.05 (4H, d, J = 8.9 Hz); ^{13}C NMR (75.5 MHz, DMSO-d_6) δ 46.5, 126.3, 127.2, 129.5, 131.1, 132.9, 133.7, 134.9, 137.3, 137.8, 152.9, 183.9; *m/z* (%) 667 (26) [M$^+$], 648 (6), 526 (100), 398 (22), 270 (12), 242 (27), 115 (24), 77 (37); Anal. Calcd. for $C_{25}H_{19}F_{10}NO_3S_3$: C, 44.98; H, 2.87; N, 2.10. Found: C, 45.05; H, 2.92; N, 2.17.

4.1.9. (3E,5E)-3,5-Bis-(4-pentafluorothiobenzylidene)-1-(toluene-4-sulfonyl)-piperidone (**2d**)

1-Tosyl-4-piperidinone (200 mg, 0.79 mmol) and 4-(pentafluorothio-)benzaldehyde (348 mg, 1.5 mmol) were dissolved in EtOH (10 mL) and conc. HCl (1 mL) was added. The reaction mixture was refluxed for 24 h. After cooling down to room temperature, the formed precipitate was collected, washed with EtOH/H_2O and dried in vacuum. Yield: 195 mg (0.29 mmol, 37%); yellow solid of m.p. 275 °C; υ_{max}(ATR)/cm^{-1} 2935, 1675, 1617, 1595, 1574, 1496, 1431, 1408, 1296, 1266, 1244, 1206, 1188, 1164, 1103, 1086, 1036, 987, 956, 937, 820, 793, 750, 729, 707, 692, 664, 635, 614, 597, 580; ^{1}H NMR (300 MHz, $CDCl_3$) δ 2.42 (3H, s), 4.52 (4H, s), 7.25 (2H, d, J = 8.1 Hz), 7.40 (4H, d, 8.8 Hz), 7.51 (2H, d, J = 8.1 Hz), 7.70 (2H, s), 7.84 (4H, d, J = 8.8 Hz); ^{13}C NMR (75.5 MHz, $CDCl_3$) δ 21.6, 46.9, 126.6, 127.6, 129.9, 130.1, 132.1, 134.0, 136.4, 137.4, 144.6, 184.2; *m/z* (%) 681 (18) [M$^+$], 662 (6), 554 (3), 526 (100), 398 (17), 270 (17), 242 (29), 155 (14), 91 (44); Anal. Calcd. for $C_{26}H_{21}F_{10}NO_3S_3$: C, 45.82; H, 3.11; N, 2.05. Found: C, 45.72; H, 3.02; N, 2.11.

4.1.10. (3E,5E)-3,5-Bis-(4-trifluoromethylbenzylidene)-1-(1-methoxybenzene-4-sulfonyl)-piperidone (**2e**)

1-(4-Methoxybenzolsulfonyl)-4-piperidinone (213 mg, 0.79 mmol) and 4-trifluoromethylbenzaldehyde (260 mg, 1.5 mmol) were dissolved in EtOH (10 mL) and conc. HCl (1 mL) was added. The reaction mixture was refluxed for 24 h. After cooling down to room temperature, the formed precipitate was collected, washed with EtOH and dried in vacuum. Yield: 140 mg (0.24 mmol, 30%); yellow solid of m.p. 244–245 °C; υ_{max}(ATR)/cm^{-1} 1675, 1614, 1594, 1576, 1499, 1468, 1442, 1414, 1341, 1321, 1300, 1263, 1243, 1160, 1138, 1124, 1111, 1091, 1068, 1037, 1015, 987, 969, 955, 941, 854, 839, 811, 799, 765, 743, 717, 692, 680, 640, 627, 618; ^{1}H NMR (300 MHz, DMSO-d_6) δ 3.87 (3H, s), 4.63 (4H, s), 7.06 (2H, d, J = 9.0 Hz), 7.45 (2H, d, J = 9.0 Hz), 7.64 (2H, s), 7.71 (4H, d, J = 8.2 Hz), 7.89 (4H, d, J = 8.2 Hz); ^{13}C NMR (75.5 MHz, DMSO-d_6) δ 46.5, 55.8, 114.6, 122.2, 125.6–125.8 (m), 128.7, 129.1, 129.6, 129.9, 130.9, 132.6, 135.6, 138.0, 163.0, 184.0; *m/z* (%) 581 (11) [M$^+$], 562 (8), 410 (100), 226 (11), 212 (28), 184 (28), 171 (42), 123 (15), 115 (25), 107 (24), 77 (23); Anal. Calcd. for $C_{28}H_{21}F_6NO_4S$: C, 57.83; H, 3.64; N, 2.41. Found: C, 57.76; H, 3.71; N, 2.46.

4.1.11. (3E,5E)-3,5-Bis-(4-pentafluorothiobenzylidene)-1-(1-methoxybenzene-4-sulfonyl)-piperidone (2f)

1-(4-Methoxybenzolsulfonyl)-4-piperidinone (213 mg, 0.79 mmol) and 4-(pentafluorothio)-benzaldehyde (348 mg, 1.5 mmol) were dissolved in EtOH (10 mL) and conc. HCl (1 mL) was added. The reaction mixture was refluxed for 24 h. After cooling down to room temperature, the formed precipitate was collected, washed with EtOH and dried in vacuum. Yield: 165 mg (0.24 mmol, 30%); yellow solid of m.p. 298–299 °C; υ_{max}(ATR)/cm^{-1} 2944, 2908, 1674, 1616, 1595, 1575, 1497, 1466, 1437, 1409, 1312, 1265, 1245, 1207, 1189, 1160, 1145, 1102, 1091, 1025, 1036, 988, 954, 937, 824, 795, 751, 730, 692, 678, 665; ^{1}H NMR (300 MHz, DMSO-d_6) δ 3.86 (3H. s), 4.63 (4H, s), 7.06 (2H, d, J = 8.8 Hz), 7.46 (2H, d, J = 8.8 Hz), 7.61 (2H, s), 7.71 (4H, d, J = 8.8 Hz), 8.05 (4H, d, J = 8.8 Hz); ^{13}C NMR (75.5 MHz, DMSO-d_6) δ 46.5, 55.8, 114.6, 126.2, 126.3, 128.6, 129.6, 131.1, 133.0, 134.9, 137.9, 152.6, 152.8, 163.1, 183.9; *m/z* (%) 697 (11) [M$^+$], 678 (8), 526 (100), 398 (18), 270 (23), 242 (26), 171 (36), 115 (15), 107 (20); Anal. Calcd. for $C_{26}H_{21}F_{10}NO_4S_3$: C, 44.76; H, 3.03; N, 2.01. Found: C, 44.68; H, 2.97; N, 2.07.

4.1.12. (3E,5E)-3,5-Bis-(4-trifluoromethylbenzylidene)-1-(1-fluorobenzene-4-sulfonyl)-piperidone (2g)

1-(4-Fluorobenzolsulfonyl)-4-piperidinone (203 mg, 0.79 mmol) and 4-trifluoromethylbenzaldehyde (260 mg, 1.5 mmol) were dissolved in EtOH (10 mL) and conc. HCl (1 mL) was added. The reaction mixture was refluxed for 24 h. After cooling down to room temperature, the formed precipitate was collected, washed with EtOH and dried in vacuum. Yield: 150 mg (0.26 mmol, 33%); yellow solid of m.p. 288–289 °C; υ_{max}(ATR)/cm^{-1} 3106, 3075, 3050, 1673, 1612, 1588, 1496, 1487, 1452, 1436, 1414, 1323, 1292, 1261, 1241, 1228, 1200, 1187, 1161, 1112, 1086, 1070, 1038, 1015, 969, 958, 951, 942, 918, 846, 837, 803, 765, 738, 710, 694, 674, 639, 617; ^{1}H NMR (300 MHz, DMSO-d_6) δ 4.69 (4H, s), 7.3–7.5 (2H, m), 7.6–7.8 (8H, m), 7.89 (4H, d, J = 8.3 Hz); ^{13}C NMR (75.5 MHz, DMSO-d_6) δ 46.5, 116.5–116.8 (m), 122.2, 124.5, 125.6–125.8 (m), 129.1, 129.6, 129.8, 130.3, 130.4, 130.5, 130.9, 131.0, 131.3, 132.3, 133.8, 135.7, 137.9, 138.5, 163.1, 166.4, 183.9; *m/z* (%) 569 (67) [M$^+$], 550 (17), 500 (15), 410 (100), 381 (23), 340 (37), 212 (52), 184 (93), 159 (40), 115 (55), 95 (43); Anal. Calcd. for $C_{27}H_{18}F_7NO_3S$: C, 56.94; H, 3.19; N, 2.46. Found: C, 57.00; H, 3.11; N, 2.51.

4.1.13. (3E,5E)-3,5-Bis-(4-pentafluorothiobenzylidene)-1-(1-fluorobenzene-4-sulfonyl)-piperidone (2h)

1-(4-Fluorobenzolsulfonyl)-4-piperidinone (203 mg, 0.79 mmol) and 4-(pentafluorothio)-benzaldehyde (348 mg, 1.5 mmol) were dissolved in EtOH (10 mL) and conc. HCl (1 mL) was added. The reaction mixture was refluxed for 20 h. After cooling down to room temperature, the formed precipitate was collected, washed with EtOH and dried in vacuum. Yield: 175 mg (0.26 mmol, 33%); yellow solid of m.p. 252 °C; υ_{max}(ATR)/cm^{-1} 1675, 1613, 1591, 1570, 1489, 1409, 1358, 1296, 1263, 1230, 1171, 1160, 1092, 1037, 981, 955, 933, 837, 823, 797, 750, 731, 712, 690, 675, 664, 636, 617, 599, 582; ^{1}H NMR (300 MHz, CDCl$_3$) δ 4.58 (4H, s), 7.1–7.2 (2H, m), 7.41 (4H, d, J = 8.8 Hz), 7.6–7.7 (2H, m), 7.70 (2H, s), 7.85 (4H, d, J = 8.8 Hz); ^{13}C NMR (75.5 MHz, DMSO-d_6) δ 46.5, 116.7, 116.9, 126.3, 130.6, 131.2, 132.7, 135.2, 137.8, 165.8, 183.9; *m/z* (%) 685 (66) [M$^+$], 666 (12), 558 (12), 526 (100), 398 (25), 270 (22), 242 (51), 115 (32), 95 (28); Anal. Calcd. for $C_{25}H_{18}F_{11}NO_3S_3$: C, 43.80; H, 2.65; N, 2.04. Found: C, 43.71; H, 2.58; N, 2.11.

4.1.14. (3E,5E)-3,5-Bis-(4-trifluoromethylbenzylidene)-1-(1-chlorobenzene-4-sulfonyl)-piperidone (2i)

1-(4-Chlorobenzolsulfonyl)-4-piperidinone (216 mg, 0.79 mmol) and 4-trifluoromethylbenzaldehyde (260 mg, 1.5 mmol) were dissolved in EtOH (10 mL) and conc. HCl (1 mL) was added. The reaction mixture was refluxed for 24 h. After cooling down to room temperature, the formed precipitate was collected, washed with EtOH and dried in vacuum. Yield: 140 mg (0.24 mmol, 30%); yellow solid of m.p. 266 °C; υ_{max}(ATR)/cm^{-1} 3094, 2822, 1674, 1614, 1584, 1478, 1453, 1413, 1367, 1319, 1300, 1264, 1237, 1188, 1169, 1140, 1113, 1094, 1068, 1039, 1013, 994, 967, 956, 937, 912, 861, 846, 825, 770, 755, 742, 736, 709, 699, 649, 636, 625; ^{1}H NMR (300 MHz, CDCl$_3$) δ 4.69 (4H, s), 7.5–7.6 (2H, m), 7.6–7.7 (4H, m), 7.72 (4H, d, J = 8.3 Hz), 7.89 (4H, d, J = 8.3 Hz); ^{13}C NMR (75.5 MHz, CDCl$_3$) δ 47.0, 122.7, 126.1–126.3 (m), 129.7, 129.9, 130.1, 130.3, 130.5, 131.4, 132.8, 136.3, 136.7, 138.4, 139.1, 184.5; *m/z* (%) 587 (23) [M$^+$], 585 (63), 516 (17), 410 (100), 381 (23), 340 (33), 212 (47), 184 (77), 115 (43), 111 (27); Anal. Calcd. for $C_{27}H_{18}ClF_6NO_3S$: C, 55.35; H, 3.10; N, 2.39. Found: C, 55.29; H, 3.20; N, 2.45.

4.1.15. (3E,5E)-3,5-Bis-(4-pentafluorothiobenzylidene)-1-(1-chlorobenzene-4-sulfonyl)-piperidone (2j)

1-(4-Chlorobenzolsulfonyl)-4-piperidinone (216 mg, 0.79 mmol) and 4-(pentafluorothio)-benzaldehyde (348 mg, 1.5 mmol) were dissolved in EtOH (10 mL) and conc. HCl (1 mL) was added. The reaction mixture was refluxed for 24 h. After cooling down to room temperature, the formed precipitate was collected, washed with EtOH and dried in vacuum. Yield: 170 mg (0.24 mmol, 30%); yellow solid of m.p. 270 °C; υ_{max}(ATR)/cm^{-1} 2933, 1677, 1617, 1587, 1475, 1409, 1354, 1266, 1243, 1189, 1168, 1096, 1037, 1016, 987, 951, 938, 823, 795, 756, 728, 693, 666; ^{1}H NMR (300 MHz, DMSO-d_6) δ 4.69 (4H, s), 7.5–7.6 (6H, m), 7.73 (4H, d, J = 8.8 Hz), 8.04 (4H, d, J = 8.8 Hz); ^{13}C NMR (75.5 MHz, DMSO-d_6) δ 46.5, 126.3, 129.2, 129.6, 131.2, 132.7, 135.1, 136.2, 137.8, 138.7, 152.9, 183.9; *m/z* (%) 703 (23) [M$^+$], 701 (46) [M$^+$], 575 (8), 527 (100), 399 (42), 270 (36), 242 (85), 115 (67), 111 (53); Anal. Calcd. for $C_{25}H_{18}ClF_{10}NO_3S_3$: C, 42.77; H, 2.58; N, 2.00. Found: C, 42.68; H, 2.66; N, 2.08.

4.1.16. (3E,5E)-3,5-Bis-(4-trifluoromethylbenzylidene)-1-(1-fluorobenzene-3-sulfonyl)-piperidone (2k)

1-(3-Fluorobenzolsulfonyl)-4-piperidinone (203 mg, 0.79 mmol) and 4-trifluoromethylbenzaldehyde (260 mg, 1.5 mmol) were dissolved in EtOH (10 mL) and conc. HCl (1 mL) was added. The reaction mixture was refluxed for 24 h. After cooling down to room temperature and 24 h in the refrigerator, the formed yellow crystals were collected, washed with EtOH and dried in vacuum. Yield: 150 mg (0.26 mmol, 33%); yellow solid of m.p. 257–258 °C; υ_{max}(ATR)/cm^{-1} 1672, 1612, 1588, 1478, 1437, 1412, 1356, 1324, 1265, 1242, 1227, 1188, 1161, 1124, 1069, 1038, 1016, 986, 952, 939, 886, 842, 807, 791, 766, 739, 703, 692, 679, 648, 625, 599; ^{1}H NMR (300 MHz, DMSO-d_6) δ 4.7–4.8 (4H, m), 7.2–7.4 (2H, m), 7.5–7.7 (4H, m), 7.7–7.8 (4H, m), 7.8–7.9 (4H, m); ^{13}C NMR (75.5 MHz, DMSO-d_6) δ 46.4, 114.0–114.4 (m), 120.7–121.0 (m), 122.2, 123.4, 125.6–125.7 (m), 129.2, 129.6, 131.0, 131.9, 132.3, 135.7, 137.8, 139.5, 160.0, 163.3, 184.0; *m/z* (%) 569 (94) [M$^+$], 550 (26), 500 (24), 410 (100), 381 (37), 358 (29), 340 (60), 226 (23), 212 (78), 184 (96), 159 (37), 115 (82), 95 (66); Anal. Calcd. for $C_{27}H_{18}F_7NO_3S$: C, 56.94; H, 3.19; N, 2.46. Found: C, 57.02; H, 3.13; N, 2.50.

4.1.17. (3E,5E)-3,5-Bis-(4-pentafluorothiobenzylidene)-1-(1-fluorobenzene-3-sulfonyl)-piperidone (2l)

1-(3-Fluorobenzenesulfonyl)-4-piperidinone (203 mg, 0.79 mmol) and 4-(pentafluorothio)-benzaldehyde (348 mg, 1.5 mmol) were dissolved in EtOH (10 mL) and conc. HCl (1 mL) was added. The reaction mixture was refluxed for 20 h. After cooling down to room temperature, the formed precipitate was collected, washed with EtOH and dried in vacuum. Yield: 170 mg (0.25 mmol, 32%); yellow solid of m.p. 206–207 °C; υ_{max}(ATR)/cm^{-1} 2933, 1683, 1618, 1595, 1498, 1479, 1438, 1412, 1353, 1306, 1272, 1239, 1224, 1185, 1160, 1101, 1083, 1070, 1041, 1041, 981, 955, 937, 892, 832, 795, 749, 731, 703, 683, 663; ^{1}H NMR (300 MHz, DMSO-d_6) δ 4.73 (4H, s), 7.3–7.4 (2H, m), 7.6–7.7 (4H, m), 7.7–7.8 (4H, m), 8.0–8.1 (4H, m); ^{13}C NMR (75.5 MHz, DMSO-d_6) δ 46.4, 114.5, 120.7, 123.6, 126.2–126.3 (m), 131.2, 131.9,

132.7, 135.0, 137.7, 139.4, 160.6–163.3 (m), 184.0; *m/z* (%) 685 (37) [M^+], 526 (100), 398 (26), 242 (45), 115 (31), 95 (33); Anal. Calcd. for $C_{25}H_{18}F_{11}NO_3S_3$: C, 43.80; H, 2.65; N, 2.04. Found: C, 43.70; H, 2.60; N, 2.09.

4.1.18. (3E,5E)-3,5-Bis-(4-trifluoromethylbenzylidene)-1-(1,2-difluorobenzene-4-sulfonyl)-piperidone (**2m**)

1-(3,4-Difluorobenzolsulfonyl)-4-piperidinone (217 mg, 0.79 mmol) and 4-trifluoromethylbenzaldehyde (260 mg, 1.5 mmol) were dissolved in EtOH (10 mL) and conc. HCl (1 mL) was added. The reaction mixture was refluxed for 24 h. After cooling down to room temperature and 24 h in the refrigerator, the formed yellow crystals were collected, washed with EtOH and dried in vacuum. Yield: 140 mg (0.24 mmol, 30%); yellow solid of m.p. 251–252 °C; υ_{max}(ATR)/cm^{-1} 1672, 1611, 1586, 1506, 1414, 1353, 1327, 1278, 1262, 1243, 1213, 1187, 1158, 1116, 1072, 1038, 1016, 985, 952, 943, 914, 887, 843, 828, 805, 776, 766, 739, 708, 699, 677, 644, 624; ^{1}H NMR (300 MHz, DMSO-d_6) δ 4.7–4.8 (4H, m), 7.4–7.5 (1H, m), 7.6–7.8 (8H, m), 7.8–7.9 (4H, m); ^{13}C NMR (75.5 MHz, DMSO-d_6) δ 46.5, 117.1–117.4 (m), 118.9–119.1 (m), 122.2, 125.4–125.7 (m), 129.2–129.6 (m), 131.0, 132.3, 134.6, 135.8, 137.8, 150.8, 184.1; *m/z* (%) 587 (87) [M^+], 568 (22), 518 (25), 410 (100), 381 (23), 340 (35), 212 (47), 184 (95), 115 (49), 100 (37); Anal. Calcd. for $C_{27}H_{17}F_8NO_3S$: C, 55.20; H, 2.92; N, 2.38. Found: C, 55.11; H, 2.86; N, 2.30.

4.1.19. (3E,5E)-3,5-Bis-(4-trifluoromethylbenzylidene)-1-(1,2-dichlorobenzene-4-sulfonyl)-piperidone (**2n**)

1-(3,4-Dichlorobenzenesulfonyl)-4-piperidinone (243 mg, 0.79 mmol) and 4-trifluoromethylbenzaldehyde (261 mg, 1.5 mmol) were dissolved in EtOH (10 mL) and conc. HCl (1 mL) was added. The reaction mixture was refluxed for 20 h. After cooling down to room temperature, the reaction mixture was kept in a refrigerator at 4 °C for 24 h, the formed precipitate was collected, washed with EtOH and dried in vacuum. Yield: 200 mg (0.32 mmol, 41%); yellow solid of m.p. 201–203 °C; υ_{max}(ATR)/cm^{-1} 3098, 1678, 1614, 1590, 1455, 1412, 1351, 1319, 1372, 1351, 1319, 1258, 1241, 1199, 1165, 1124, 1109, 1069, 1031, 1015, 982, 966, 956, 928, 891, 846, 821, 800, 766, 739, 703, 686, 654, 630; ^{1}H NMR (300 MHz, DMSO-d_6) δ 4.78 (4H, s), 7.4–7.5 (1H, m), 7.6–7.7 (3H, m), 7.7–7.8 (4H, m), 7.8–8.0 (5H, m); ^{13}C NMR (75.5 MHz, DMSO-d_6) δ 46.5, 122.2, 125.7, 127.3, 128.8, 128.9, 129.2, 129.4, 129.6, 131.1, 131.8, 132.1, 132.4, 135.9, 136.8, 137.7, 137.9, 183.9; *m/z* (%) 621 (17) [M^+], 619 (32) [M^+], 602 (3), 600 (4), 552 (6), 550 (8), 410 (100), 381 (12), 340 (21), 212 (28), 184 (48), 145 (35), 115 (45); Anal. Calcd. for $C_{27}H_{17}Cl_2F_6NO_3S$: C, 52.27; H, 2.76; N, 2.26. Found: C, 52.19; H, 2.69; N, 2.20.

4.1.20. (3E,5E)-3,5-Bis-(4-pentafluorothiobenzylidene)-1-(1,2-dichlorobenzene-4-sulfonyl)-piperidone (**2o**)

1-(3,4-Dichlorobenzenesulfonyl)-4-piperidinone (243 mg, 0.79 mmol) and 4-(pentafluorothio)-benzaldehyde (348 mg, 1.5 mmol) were dissolved in EtOH (10 mL) and conc. HCl (1 mL) was added. The reaction mixture was refluxed for 20 h. After cooling down to room temperature, the formed precipitate was collected and washed with EtOH. The yellow precipitate was recrystallized from EtOH. Yield: 190 mg (0.26 mmol, 33%); yellow solid of m.p. 225–226 °C; υ_{max}(ATR)/cm^{-1} 1675, 1615, 1589, 1495, 1450, 1434, 1407, 1374, 1357, 1292, 1265, 1243, 1188, 1171, 1141, 1097, 1035, 987, 950, 940, 891, 821, 792, 750, 728, 702, 692, 678, 666, 653, 627; ^{1}H NMR (300 MHz, DMSO-d_6) δ 4.78 (4H, s), 7.49 (1H, d, J = 8.5 Hz), 7.61 (2H, s), 7.7–7.8 (5H, m), 7.84 (1H, d, J = 8.5 Hz), 8.0–8.1 (4H, m); ^{13}C NMR (75.5 MHz, DMSO-d_6) δ 46.5, 126.3, 127.3, 129.0, 131.2, 132.4, 132.5, 135.2, 136.8, 137.6, 137.9, 152.9, 183.8; *m/z* (%) 737 (17) [M^+], 735 (24) [M^+], 718 (3), 716 (4), 610 (4), 608 (6), 526 (100), 398 (31), 270 (25), 242 (58), 145 (43), 115 (68); Anal. Calcd. for $C_{25}H_{17}Cl_2F_{10}NO_3S_3$: C, 40.77; H, 2.33; N, 1.90. Found: C, 40.70; H, 2.39; N, 1.85.

4.2. Leishmania major cell isolation, culture conditions, and assays

Promastigotes of *L. major* were isolated from a Saudi patient (February 2016) and maintained at 26 °C in Schneider's Drosophila medium (Invitrogen, USA) containing 10% heat inactivated fetal bovine serum (FBS, Invitrogen, USA) and antibiotics in a tissue culture flask with weekly transfers. Promastigotes were cryopreserved in liquid nitrogen at concentrations of 3 × 10^6 parasite/mL. Virulent *L. major* parasites were maintained by passing in female BALB/c mice by injecting hind footpads with 1x10^6 stationary-phase promastigotes. *l. major* amastigotes were isolated from the mice after 8 weeks. Isolated amastigotes were converted to promastigotes by cultivation at 26 °C in Schneider's medium supplemented with antibiotics and 10% FBS. Amastigote-derived promastigotes, which had undergone less than five *in vitro* passages, were used for infection. BALB/c mice (male and female individuals) were obtained from Pharmaceutical College, King Saud University, Kingdom of Saudi Arabia, and maintained in specific pathogen-free facilities. The handling of the laboratory animals followed the instructions and rules of the committee of research ethics, Deanship of Scientific Research, Qassim University, permission number 20–03-20.

L. major promastigotes from logarithmic-phase were cultured in phenol red-free RPMI 1640 medium (Invitrogen, USA) with 10% FBS and suspended on 96-wells plates to yield 10^6 cells mL^{-1} (200 μL/well) after counting by a hemocytometer. Compounds were added to the wells, obtaining final concentrations of 50, 25, 12.5, 6.25, 3.13, 1.65, and 0.75 μg mL^{-1}. Negative controls contained cultures with DMSO (1%) devoid of test compound and positive control wells contained cultures with decreasing concentrations of amphotericin B (50, 25, 12.5, 6.25, 3.13, 1.65, 0.75 μg mL^{-1}) as active reference compound. After incubation at 26 °C for 72 h, the number of viable promastigotes was assessed by colorimetric method (tetrazolium salt colorimetric assay, MTT). The formed colored formazan was isolated and solubilized by addition of a detergent solution. The samples were analysed by using an ELISA reader at 570 nm. EC_{50} values were calculated from three independent experiments [46].

For evaluation of the activity against amastigotes in macrophages, peritoneal macrophages were collected from female BALB/c mice (6–8 weeks of age) by aspiration. 5 × 10^4 cells/well were placed into 96-wells plates containing phenol red-free RPMI 1640 medium with 10% FBS and were incubated to promote cell adhesion at 37 °C for 4 h in 5% CO_2 atmosphere. Thereafter, the medium was discarded and the cells were washed with phosphate buffered saline (PBS). *L. major* promastigotes solution (200 μL at a ratio of 10 promastigotes : 1 macrophage in RPMI 1640 medium with 10% FBS) was added to each well and the plates were incubated for 24 h at 37 °C in humidified 5% CO_2 atmosphere to enable macrophage infection and amastigote differentiation. The infected cells were washed three times with PBS to remove the free promastigotes and overlaid with fresh phenol red-free RPMI 1640 medium containing test compounds (50, 25, 12.5, 6.25, 3.13, 1.65, and 0.75 μg mL^{-1}) whereupon the cells were incubated at 37 °C for 72 h in humidified 5% CO_2 atmosphere. Cultures solely containing DMSO (1%) were used as negative controls while wells containing cultures with decreasing concentrations of amphotericin B (reference compound, 50, 25, 12.5, 6.25, 3.13, 1.65, and 0.75 μg mL^{-1}) were used as positive control. The percentage of infected macrophages was evaluated microscopically after the removal of the medium, washing, fixation, and Giemsa staining of the cells. Calculated EC_{50} values were obtained from three independent experiments [46].

4.3. Toxoplasma gondii cell line, culture conditions, and assay

Serial passages of cells of the Vero cell line (ATCC® CCL81™, USA) were applied for the cultivation of *T. gondii* tachyzoites of the RH strain (a gift from Dr. Saeed El-Ashram, State Key Laboratory for Agrobiotechnology, China Agricultural University, Bejing, China). Vero cells were cultured by using complete RPMI 1640 medium with heat-

inactivated 10% FBS in a humidified 5% CO_2 atmosphere at 37 °C. 96-Well plates (5×10^3 cells/well in 200 μL RPMI 1640 medium) were used for the cultivation of the Vero cells and then incubated at 37 °C and 5% CO_2 for one day, followed by removal of medium and washing the cells with PBS. Then, RPMI 1640 medium containing 2% FBS and *T. gondii* tachyzoites (RH strain) was given to the cells at a ratio of 5 (parasite) : 1 (Vero cells). After incubation at 37 °C and 5% CO_2 for 5 h, cells were washed with PBS and then treated as described below.

Control: RPMI 1640 medium containing DMSO (1%)

Experimental: Medium + compounds (dissolved in DMSO) (50, 25, 12.5, 6.25, 3.13, 1.65, and 0.75 μg mL^{-1}).

After incubation at 37 °C and 5% CO_2 for 72 h, the cells were washed with PBS, fixed in 10% formalin and stained with 1% toluidine blue. Examination of the cells and determination of the infection index (number of cells infected from 200 cells tested) of *T. gondii* were carried out with an inverted photomicroscope. The following equation was used for the calculation of the inhibition in %:

Inhibition (%) = (I Control - I Experimental)/(I Control) × 100

where, I Control refers to the infection index of untreated cells and I Experimental refers to the infection index of cells treated with test compounds.

Then effects of test compounds on parasite growth were expressed as EC_{50} (effective concentration at 50%) values. EC_{50} values were obtained from three independent experiments [46,47].

4.4. In vitro cytotoxicity assay

MTT assays were carried out for a cytotoxicity evaluation of the test compounds. Briefly, Vero cells were cultured in 96-well plates (5×10^3 cells/well/200 μL) for 24 h in RPMI 1640 medium with 10% FBS and 5% CO_2 at 37 °C. Cells were washed with PBS, followed by treatment with test compounds for 72 h at varying concentrations (50, 25, 12.5, 6.25, 3.13, 1.65, and 0.75 μg mL^{-1}) in 10% FBS medium. Cells treated solely with medium in 2% FBS were used as negative control. The supernatant was discarded and 50 μL RPMI 1640 medium containing 14 μL MTT (5 mg mL^{-1}) was added and the cells were incubated for 4 h. The supernatant was removed again and 150 μL DMSO was added in order to dissolve the formed formazan. A FLUOstar OPTIMA spectrophotometer was applied for colorimetric analysis ($\lambda = 540$ nm). The cytotoxicity was expressed by IC_{50} values (concentration which caused a 50% reduction in viable cells). IC_{50} values were calculated from three independent experiments [46,48].

4.5. Computational methods

The Gaussian 16 program was used for DFT calculations. Geometry optimizations (with default optimization criteria) were carried out for all structures described in this paper [49]. Full optimization was performed for the gas phase, using B3LYP and the polarized valence-triple-ζ basis set (6–311 g(d,p)) [50]. To include dispersion effects, we used the recently developed nonlocal van der Waals functional, B3LYP-D3.

To obtain validated QSAR models, molecular descriptors were determined using the software IBM SPSS Statistics 19.0. QSAR properties encoded different information about scale, hydrophilicity, electronic and topological properties calculated using HyperChem software (version 8.0.3) [51,52].

Molecular docking was performed with AutoDock Version 4.2 [53]. For preparation of the protein and the ligands for docking, AutoDock Tools (ADT) was used [53,54]. The software source was The Scripps Research Institute, San Diego, CA, USA.

The docking procedure has been described earlier [55,56]. The PDB file – 1E92 was downloaded from the Protein Data Bank for the three dimensional structure of pteridine reductase – subunit A (PTR1A). Structures of ligands, **1i** and EF24, were generated with ChemSketch. Conversion of structure files to pdb formats was done with Open Babel software. Nonpolar hydrogens were merged and Gasteiger partial charges were assigned to all atoms. In applying torsions in ligands all rotatable bonds were rotated. The ligands were made flexible and the protein was kept rigid. PDBQT files (file format that contains partial charges and torsion records along with atom coordinates) were written for the protein and each ligand and were used as input files for docking experiments.

Standard docking procedures for a rigid protein and a flexible ligand were used as per user guide for AutoDock.4.2. Briefly, using AutoGrid a grid of 60x60x60 points in ×, y, and z directions was built with grid points spaced at 0.375 Å. Electrostatic maps were calculated by using a distance dependent function of dielectric constants. All other parameters were set as default. Docking simulations were performed by employing Lamarckian Genetic Algorithm (LGA). The implementation of LGA included the creation of an initial population of 150 individuals, for which random torsions were applied. In each docking run, a maximum of 2,500,000 energy evaluations was performed. For either of the two ligands, at least 20 such runs were performed. The best binding modes for each ligand were analyzed with LigPlot+, ADT and RasMol (Roger Sayle) programs [57].

Declaration of Competing Interest

The authors declare that they have no known competing financial interests or personal relationships that could have appeared to influence the work reported in this paper.

Acknowledgements

We are grateful to the College of Applied Health Sciences at Ar Rass, Qassim University.

Appendix A. Supplementary data

Supplementary data to this article can be found online at https://doi.org/10.1016/j.bioorg.2021.105099.

References

[1] A. Goel, A.B. Kunnumakkara, B.B. Aggarwal, Curcumin as "curecumin": from kitchen to clinic, Biochem. Pharmacol. 75 (2008) 787–809.
[2] B. Bachmeier, A.G. Nerlich, C.M. Iancu, M. Cilli, E. Schleicher, R. Vene, R. Dell'Eva, M. Jochum, A. Albini, U. Pfeffer, The chemopreventive polyphenol curcumin prevents hematogenous breast cancer metastases in immunodeficient mice, Cell. Physiol. Biochem. 19 (2007) 137–152.
[3] A. Bharti, N. Donato, S. Singh, B.B. Aggarwal, Curcumin (diferuloylmethane) down-regulates the constitutive activation of nuclear factor-kappa B and IkappaBalpha kinase in human multiple myeloma cells, leading to suppression of proliferation and induction of apoptosis, Blood 101 (2003) 1053–1062.
[4] J. Woo, Y.H. Kim, Y.J. Choi, D.G. Kim, K.S. Lee, J.H. Bae, D.S. Min, J.S. Chang, Y. J. Jeong, Y.H. Lee, J.W. Park, T.K. Kwon, Molecular mechanisms of curcumin-induced cytotoxicity: Induction of apoptosis through generation of reactive oxygen species, down-regulation of Bcl-XL and IAP, the release of cytochrome c and inhibition of Akt, Carcinogenesis 24 (2003) 1199–1208.
[5] S. Plummer, K.A. Holloway, M.M. Manson, R.J. Munks, A. Kaptein, S. Farrow, L. Howells, Inhibition of cyclo-oxygenase 2 expression in colon cells by the chemopreventive agent curcumin involves inhibition of NF-kappaB activation via the NIK/IKK signalling complex, Oncogene 18 (1999) 6013–6020.
[6] L.I. Lin, Y.F. Ke, Y.C. Ko, J.K. Lin, Curcumin inhibits SK-Hep-1 hepatocellular carcinoma cell invasion in vitro and suppresses matrix metalloproteinase-9 secretion, Oncology 55 (1998) 349–353.
[7] N. Dhillon, B.B. Aggarwal, R.A. Newman, R.A. Wolff, A.B. Kunnumakkara, J. L. Abbruzzese, C.S. Ng, V. Badmaev, R. Kurzrock, Phase II trial of curcumin in patients with advanced pancreatic cancer, Clin. Cancer Res. 14 (2008) 4491–4499.
[8] D. Praditya, L. Kirchhoff, J. Brüning, H. Rachmawati, J. Steinmann, E. Steinmann, Anti-infective properties of the golden spice curcumin, Front. Microbiol. 10 (2019) 912.
[9] R.K. Kesharwani, K. Misra, D.B. Singh, Perspectives and challenges of tropical medicinal herbs and modern drug discovery in the current scenario, Asian Pac. J. Trop. Med. 12 (2019) 1–7.
[10] M. Shahiduzzaman, A. Daugschies, Curcumin: a natural herb extract with antiparasitic properties, in: H. Mehdorn (Ed.), Nature helps: How Plants and Other Organisms Contribute to Solve Health Problems, Springer-Verlag, Berlin, Heidelberg, 2011, pp. 141–152.

[11] K. Cheraghipour, A. Marzban, B. Ezatpour, S. Khanizadeh, J. Koshki, Antiparasitic properties of curcumin: a review, AIMS Agric. Food 4 (2019) 1–18.

[12] M. Fouladvand, A. Barazesh, R. Tahmasebi, Evaluation of in vitro antileishmanial activity of curcumin and its derivatives' gallium curcumin, indium curcumin and diacethyl curcumiń, Eur. Rev. Med. Pharmacol. Sci. 17 (2013) 3306–3308.

[13] Y.-K. Goo, J. Yamagishi, A. Ueno, M.A. Terkawi, G.O. Aboge, D. Kwak, Y. Hong, D.-I. Chung, M. Igarashi, Y. Nishikawa, X. Xuan, Characterization of *Toxoplasma gondii* glyoxalase 1 and evaluation of inhibitory effects of curcumin on the enzyme and parasite culture, Parasites Vectors 8 (2015) 654.

[14] I. Al Nasr, F. Ahmed, F. Pullishery, S. El-Ashram, V.V. Ramaiah, Toxoplasmosis and anti-*Toxoplasma* effects of medicinal plant extracts – a mini-review, Asian Pac, J Trop. Med. 9 (2016) 730–734.

[15] http://www.who.int/mediacentre/factsheets/fs375/en/; Accessed November 12, 2020.

[16] K. van Bocxlaer, D. Caridha, C. Black, B. Vesely, S. Leed, R.J. Sciotti, G.-J. Wijnant, V. Yardley, S. Braillard, C.E. Mowbray, J.-R. Ioset, S.L. Croft, Novel benzoxaborole, nitroimidazole and aminopyrazoles with activity against experimental cutaneous leishmaniasis, IJP: Drugs Drug Resist. 11 (2019) 129–138.

[17] I. Bennis, L. Belaid, V. de Brouwere, H. Filali, H. Sahibi, M. Boelart,'The mosquitoes that destroy your face': social impact of cutaneous leishmaniasis in south-eastern Morocco, a quality study, PLoS ONE 12 (2017), e0189906.

[18] M. Kassi, A. Afghan, R. Rehman, P.M. Kasi, Marring leishmaniasis: the stigmatization and the impact of cutaneous leishmaniasis in Pakistan and Afghanistan, PLoS Negl. Trop. Dis. 2 (2008), e259.

[19] A. Vyas, P. Dandawate, S. Padhye, A. Ahmad, F. Sarkar, Perspectives on new synthetic curcumin analogs and their potential anticancer properties, Curr. Pharm. Des. 19 (2013) 2047–2069.

[20] A.L. Kasinski, Y. Du, S.L. Thomas, J. Zhao, S.-Y. Sun, F.R. Khuri, C.-Y. Wang, M. Shoji, A. Sun, J.P. Snyder, D. Liotta, H. Fu, Inhibition of IκB kinase-nuclear factor-κB signalling pathway by 3,5-bis(2-fluorobenzylidene)piperidin-4-one (EF24), a novel monoketone analog of curcumin, Mol. Pharmacol. 74 (2008) 654–661.

[21] D. Subramaniam, R. May, S.M. Sureban, K.B. Lee, R. George, P. Kuppusamy, R. P. Ramanujam, K. Hideg, B.K. Dieckgraefe, C.W. Houchen, S. Anant, Diphenyl difluoroketone: A curcumin derivative with potent in vivo anticancer activity, Cancer Res. 68 (2008) 1962–1969.

[22] J.M. Reid, S.A. Buhrow, J.A. Gilbert, L. Jia, M. Shoji, J.P. Snyder, M.M. Ames, Mouse pharmacokinetics and metabolism of the curcumin analog, 4-piperi-done,3,5,-bis[(2-fluorophenyl)methylene]-acetate(3E,5E) (EF-24; NSC 716993), Cancer Chemother. Pharmacol. 73 (2014) 1137–1146.

[23] F. Schmitt, M. Gold, G. Begemann, I. Andronache, B. Biersack, R. Schobert, Fluoro and pentafluorothio analogs of the antitumoral curcuminoid EF24 with superior antiangiogenic and vascular-disruptive effects, Bioorg. Med. Chem. 25 (2017) 4894–4903.

[24] F. Schmitt, D. Subramaniam, S. Anant, S. Padhye, G. Begemann, R. Schobert, B. Biersack, Halogenated bis(methoxy-benzylidene)-4-piperidone curcuminoids with improved anticancer activity, ChemMedChem 13 (2018) 1115–1123.

[25] J.R. Dimmock, M.P. Padmanilayam, G.A. Zello, K.H. Nienaber, T.M. Allen, C. L. Santos, E. De Clercq, J. Balzarini, E.K. Manavathu, J.P. Stables, Cytotoxic analogues of 2,6-bis(arylidene)cyclohexanones, Eur. J. Med. Chem. 38 (2003) 169–177.

[26] K.-L. Tan, A. Ali, Y. Du, H. Fu, H.-X. Jin, T.-M. Chin, M. Khan, M.-L. Go, Synthesis and evaluation of bisbenzylidenedioxotetrahydrothiopranones as activators of endoplasmic reticulum (ER) stress signaling pathways and apoptotic cell death in acute promyelocytic leukemic cells, J. Med. Chem. 57 (2014) 5904–5918.

[27] A. Thakur, S. Manohar, C.E.V. Gerena, B. Zayas, V. Kumar, S.V. Malhotra, D. S. Rawat, Novel 3,5-bis(arylidene)-4-piperidone based monocarbonyl analogs of curcumin: anticancer activity and mode of action study, Med. Chem. Commun. 5 (2014) 576–586.

[28] S. Altomonte, M. Zanda, Synthetic chemistry and biological activity of pentafluorosulphanyl (SF_5) organic molecules, J. Fluor. Chem. 143 (143) (2012) 57–93.

[29] T. Mo, X. Mi, E.E. Milner, G.S. Dow, P. Wipf, Synthesis of an 8-pentafluorosulfanyl analog of the antimalarial agent mefloquine, Tetrahedron Lett. 51 (2010) 5137–5140.

[30] S. Piras, A. Carta, I. Briguglio, P. Corona, G. Paglietti, R. Luciana, M.P. Costi, S. Ferrari, 2-[-Alkyl(R-phenyl)-aminomethyl]-3-phenyl-7-trifluoromethylquinazolines as anticancer agents inhibitors of folate enzymes, Eur. J. Med. Chem. 75 (2014) 169–183.

[31] P. Linciano, C. Pozzi, L. dello Iacono, F. di Pisa, G. Landi, A. Bonucci, S. Gul, M. Kuzikov, B. Ellinger, G. Witt, N. Santarem, C. Baptista, C. Franco, C.B. Moraes, W. Müller, U. Wittig, R. Luciani, A. Sesenna, A. Quotadamo, S. Ferrari, I. Pöhner, A. Corderio-da-Silva, S. Mangani, L. Costantino, M.P. Costi, Enhancement of benzothiazoles as pteridine reductase-1 inhibitors for the treatment of trypanosomatidic infections, J. Med. Chem. 62 (2019) 3989–4012.

[32] J. Kaur, P. Kumar, S. Tyagi, R. Pathak, S. Batra, P. Singh, N. Singh, In silico screening structure-activity relationship, and biologic evaluation of selective pteridine reductase inhibitors targeting visceral leishmaniasis, Antimicrob. Agents Chemother. 55 (2011) 659–666.

[33] A. Cavazzuti, G. Paglietti, W.N. Hunter, F. Gamarro, S. Piras, M. Loriga, S. Alleca, P. Corona, K. McLuskey, L. Tulloch, F. Gibellini, S. Ferrari, M.P. Costi, Discovery of potent pteridine reductase inhibitors to guide antiparasite drug development, PNAS 105 (2008) 1448–1453.

[34] C. Mendoza-Martínez, J. Correa-Basurto, R. Nieto-Meneses, A. Márquez-Navarro, R. Aguilar-Suárez, M.D. Montero-Cortes, B. Nogueda-Torres, E. Suárez-Contreras, N. Galindo-Sevilla, A. Rjas-Rojas, A. Rodriguez-Lezama, F. Hernández-Luis, Design, synthesis and biological evaluation of quinazoline derivatives as anti-trypanosomatid and anti-plasmodial agents, Eur. J. Med. Chem. 96 (2015) 296–307.

[35] K. Griewank, C. Gazeau, A. Eichhorn, E. von Strebut, Miltefosine efficiently eliminates *Leishmania major* amastigotes from infected murine dendritic cells without altering their immune functions, Antimicrob. Agents Chemother. 54 (2010) 652–659.

[36] L.A. Sarouey, K. Khanaliha, P. Rahimi-Moghaddam, S. Khorrami, M.S. Dayer, F. Tabataie, *In vitro* effects of ketotifen and cromolyn sodium on promastigotes and amastigotes of *Leishmania major*, Jundishapur J. Microbiol. 12 (2019), e82389.

[37] C. Cohen, G. Perrault, C. Voltz, R. Steinberg, P. Soubrié, SR141716, a central cannabinoid (CB(1)) receptor antagonist, blocks the motivational and dopamine-releasing effects of nicotine in rats, Behav. Pharmacol. 13 (2007) 451–463.

[38] C. Castellano, C. Rossi-Arnaud, V. Cestari, M. Costanzi, Cannabinoids and memory: animal studies, Curr. Drug Targets CNS Neurol. Disord. 2 (2003) 389–402.

[39] B.L. Hungund, B.S. Basavarajappa, C. Vadasz, G. Kunos, F.R. de Fonseca, G. Colombo, S. Serra, L. Parsons, G.F. Koob, Ethanol, endocannabinoids, and the cannabinoidergic signaling system, Alcoholism Clin. Exp. Res. 26 (2002) 565–574.

[40] M. Ghamri, D. Harkati, S. Belaidi, S. Boudergua, R. Ben Said, R. Linguerri, G. Chambaud, M. Hochlaf, Carbazole derivatives containing chalcone analogues targeting topoisomerase II inhibition: first principles, characterization and QSAR modelling, Spectrochim. Acta A: Biomol. Spectr. 242 (2020), 118724.

[41] G. Pèpe, G. Guiliani, S. Loustalet, P. Halfon, Hydration free energy a fragmental model and drug design, Eur. J. Med. Chem. 37 (2002) 865–872.

[42] T. Salah, S. Belaidi, N. Melkemi, N. Tchouar, Molecular geometry, electronic properties, MPO methods and structure activity/property relationship studies of 1,3,4-thiadiazole derivatives by theoretical calculations, Rev. Theoret. Sci. 3 (2015) 355–364.

[43] B. Nare, L.W. Hardy, S.M. Beverley, The roles of pteridine reductase 1 and dihydrofolate reductase-thymidylate synthase in pteridine metabolism in the protozoan parasite *Leishmania major*, J. Biol. Chem. 272 (1997) 13883–13891.

[44] D.G. Gourley, A.W. Schüttelkopf, G.A. Leonard, J. Luba, L.W. Hardy, S.M. Beverley, W.N. Hunter, Pteridine reductase mechanism correlates pterin metabolism with drug resistance in trypanosomatid parasites, Nat. Struct. Biol. 8 (2001) 521–525.

[45] H. Istanbullu, G. Bayraktar, H. Akbaba, I. Cavus, G. Coban, B.D. Butuner, A. A. Kilimcioglu, A. Ozbilgin, V. Alptuzun, E. Erciyas, Design, synthesis, and in vitro biological evaluation of novel thiazolopyrimidine derivatives as antileishmanial compounds, Arch. Pharm. 353 (2020), e1900325.

[46] I. Al Nasr, J. Jentzsch, I. Winter, R. Schobert, K. Ersfeld, W. Koko, A. Mujawah, T. Khan, B. Biersack, Antiparasitic activities of new lawsone Mannich bases, Arch. Pharm. Chem. Life Sci. 352 (2019) 1900128.

[47] K.M. Choi, J. Gang, J. Yun, Anti-*Toxoplasma gondii* RH strain activity of herbal extracts used in traditional medicine, Int. J. Antimicrob. Agents 32 (2008) 360–362.

[48] W.S. Koko, M.A. Mesaik, S. Yousaf, M. Galal, M.I. Choudhary, *In vitro* immunomodulating properties of selected Sudanese medicinal plants, J. Ethnopharmacol. 118 (2008) 26–34.

[49] M.J. Frisch, G.W. Trucks, H.B. Schlegel, G.E. Scuseria, M.A. Robb, J.R. Cheeseman, G. Scalmani, V. Barone, G.A. Petersson, H. Nakatsuji, X. Li, M. Caricato, A.V. Marenich, J. Bloino, B.G. Janesko, R. Gomperts, B. Mennucci, H.P. Hratchian, J.V. Ortiz, A.F. Izmaylov, J.L. Sonnenberg, D. Williams-Young, F. Ding, F. Lipparini, F. Egidi, J. Goings, B. Peng, A. Petrone, T. Henderson, D. Ranasinghe, V.G. Zakrzewski, J. Gao, N. Rega, G. Zheng, W. Liang, M. Hada, M. Ehara, K. Toyota, R. Fukuda, J. Hasegawa, M. Ishida, T. Nakajima, Y. Honda, O. Kitao, H. Nakai, T. Vreven, K. Throssell, J.A. Montgomery Jr., J.E. Peralta, F. Ogliaro, M.J. Bearpark, J.J. Heyd, E.N. Brothers, K.N. Kudin, V.N. Staroverov, T.A. Keith, R. Kobayashi, J. Normand, K. Raghavachari, A.P. Rendell, J.C. Burant, S.S. Iyengar, J. Tomasi, M. Cossi, J.M. Millam, M. Klene, C. Adamo, R. Cammi, J.W. Ochterski, R.L. Martin, K. Morokuma, O. Farkas, J.B. Foresman, D.J. Fox, Gaussian 16, Revision B.01, Gaussian Inc. Wallingford CT, 2016.

[50] M.W. Wong, P.M.W. Gill, R.H. Nobes, L. Radom, 6–311G (MC)(d, p): a second-row analogue of the 6–311G (d, p) basis set: calculated heats of formation for second-row hydrides, J. Phys. Chem. 92 (1988) 4874–4880.

[51] S. Corporate, SPSS-X User's Guide, McGraw-Hill Inc, New York, 1985.

[52] O. Ivanciuc, HyperChem release 4.5 for windows, J. Chem. Inf. Comput. Sci. 36 (1996) 612–614.

[53] G.M. Morris, R. Huey, W. Lindstrom, M.F. Sanner, R.K. Belew, D.S. Goodsell, A. J. Olson, AutoDock4 and AutoDockTools4: automated docking with selective receptor flexibility, J. Comput. Chem. 30 (2009) 2785–2791.

[54] M.F. Sanner, Python: a programming language for software integration and development, J. Mol. Graph. Model. 17 (1999) 57–61.

[55] Y. Hobani, A. Jerah, A. Bidwai, A comparative molecular docking study of curcumin and methotrexate to dihydrofolate reductase, Bioinformation 13 (2017) 63–66.

[56] A. Jerah, Y. Hobani, B.V. Kumar, A. Bidwai, Curcumin binds in silico to anti-cancer drug target enzyme MMP-3 (human stromelysin-1) with affinity comparable to two known inhibitors of the enzyme, Bioinformation 11 (2015) 387–392.

[57] R.A. Sayle, E.J. Milner-White, RASMOL: biomolecular graphics for all, Trends Biochem. Sci. 20 (1995) 374–376.